Annu. Rev. Biochem. 1999. 68:687–728

STRUCTURAL MECHANISM OF MUSCLE CONTRACTION

M. A. Geeves
Department of Biosciences, University of Kent, Canterbury, CT2 7NJ, United Kingdom; e-mail: m.a.geeves@ukc.ac.uk

K.C. Holmes
Max Planck Institute for Medical Research, 69120 Heidelberg, Germany; e-mail: holmes@mpimf-heidelberg.mpg.de

Key Words actin, myosin, structure, muscle contraction, swinging cross bridge, molecular mechanism, kinetics, mutations

■ **Abstract** X-ray crystallography shows the myosin cross-bridge to exist in two conformations, the beginning and end of the "power stroke." A long lever-arm undergoes a 60° to 70° rotation between the two states. This rotation is coupled with changes in the active site (OPEN to CLOSED) and phosphate release. Actin binding mediates the transition from CLOSED to OPEN. Kinetics shows that the binding of myosin to actin is a two-step process which affects ATP and ADP affinity. The structural basis of these effects is not explained by the presently known conformers of myosin. Therefore, other states of the myosin cross-bridge must exist. Moreover, cryoelectronmicroscopy has revealed other angles of the cross-bridge lever arm induced by ADP binding. These structural states are presently being characterized by site-directed mutagenesis coupled with kinetic analysis.

CONTENTS

INTRODUCTION

Scope of Review

Movement in muscle is generated by the myosin cross-bridges, which interact cyclically with thin (actin) filaments and transport them past the myosin thick filaments. During the process ATP is hydrolyzed. In the last five years protein crystallography of the myosin cross-bridge has given new insight into these processes. Kinetics, spectroscopy, genetic analysis, in vitro motility assays, and chemical cross-linking have also played important roles (see 1–15).

The myosin cross-bridge is a molecular machine with communicating functional units: the actin-binding site, the nucleotide-binding site/hydrolysis, and the converter/lever arm, which appears to amplify the small changes at the active site into the large changes needed to transport actin past myosin. These function-

alities were recognized and explored experimentally long before the atomic structures were known: Atomic structures now embody such concepts with machine-like linkages fabricated from polypeptide chains.

We first summarize the structural results. Then we explore the behavior of the individual functional units in structural terms (so far as this is presently possible) and how these functionalities appear to be linked. Mutational studies begin to show how such pathways of communication can be disrupted (16). Moreover, the natural variants of myosin—smooth/fast/slow/heart/nonmuscle myosin II and other myosins—provide new insights into both structure and function. For example, alternate splicing in *Drosophila* myosins identifies areas that are important for defining function (17).

The myosin cross-bridge may be cleaved off the myosin molecule as a soluble molecule (myosin S1, ~120,000 Da) that contains three polypeptide chains, one heavy and two light. Myosin S1 is a fully competent actin-activated ATPase that transports actin in vitro motility assays. Moreover, in the absence of nucleotide, myosin S1 forms a tight (rigor) bond to actin filaments. Biochemical and structural investigations have therefore been concentrated on myosin S1 and its interactions with actin as a minimal model for muscle. However, since it is no longer attached to the myosin thick filament, myosin S1 cannot be an adequate model for a strained cross-bridge. Thus data from muscle fibers (e.g. the dependence of phosphate affinity on strain) must also be considered.

There is a rich literature on the kinetics of myosin S1 ATPase. Changes in the intrinsic protein fluorescence play a central role in signaling conformational states of myosin and linking these to catalytic events. To make full use of these results we need to establish the correspondence between the crystallographic states and the kinetic states. Moreover, the structural data urge a reinterpretation of these kinetic schemes and oblige one to see these different processes in a wider context.

Clearly, the interaction of S1 with the actin filament is of central importance. Unfortunately, here the structural data are of limited precision. However, by consideration of the kinetics of the actomyosin interaction, one is led to the conclusion that there must be more myosin states than the two which have so far been revealed by protein crystallography. Finally, one can hypothesize about the nature of the missing state and the way the cross-bridge states might interconvert in active muscle.

The Swinging Cross-Bridge

The swinging–cross-bridge theory for muscle contraction envisages that the myosin cross-bridge binds to the actin filament in an initial conformation and then undergoes a swinging motion that "rows" the actin filament along (10). Myosin is a product-inhibited ATPase with an active site and mechanism similar to that of the G-proteins (18). The ATPase is strongly stimulated by binding to actin, which is a nucleotide exchange factor for myosin. In the absence of nucleotide the myosin cross-bridge binds tightly to the actin filament to form the "strong" or "rigor" complex (Figure 1). The binding of ATP to the ATPase site on

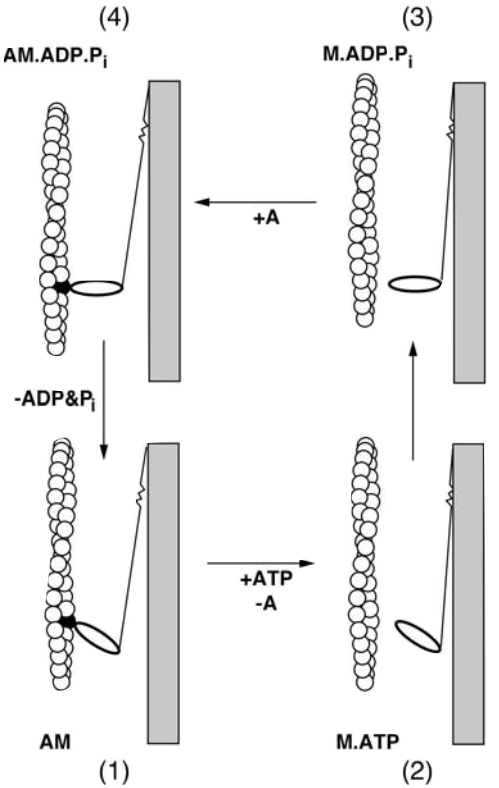

Figure 1 The Lymn-Taylor cycle (19). The myosin cross-bridge is bound to actin in the rigor, 45° "down" position (state *1*). ATP binds, which leads to very fast dissociation from actin (state *2*). The hydrolysis of ATP to ADP and P_i leads to a return of the myosin cross-bridge to the 90° "up" position, whereupon it rebinds to actin (state *4*). This leads to release of the products and return to state 1. In the last transition, actin is "rowed" past myosin.

the myosin cross-bridge rapidly dissociates the actomyosin complex; myosin then hydrolyzes ATP and forms a stable myosin-products complex ($ADP.P_i$); actin recombines with this complex and dissociates the products, thereby forming the original actin-myosin complex (19). After recombining with actin, the cross-bridge undergoes a conformational change allowing the products of hydrolysis to be released, which also brings about the rowing-like stroke (this elemental event is referred to as the "power stroke").

Although the swinging–cross-bridge hypothesis of muscle contraction features in most textbooks, it has in fact proved remarkably difficult to visualize a bridge during the swing. Finally, after many years of effort involving the development of new X-ray sources (see 20 for historical review), time-resolved X-ray

fiber diagrams from contracting frog muscle provided evidence of cross-bridge movement (21, 22). However, such experiments do not have sufficient resolution to define the cross-bridge movement in any detail. Owing to a number of spectroscopic and structural observations (see 23), the swinging cross-bridge was modified into a swinging-lever arm hypothesis in which the bulk of the cross-bridge was envisaged to bind to actin without rolling on the surface during the power stroke (as had initially been suggested); large movements were envisaged as coming from the distal (C-terminal) part of the myosin cross-bridge moving as a lever arm (Figure 2).

A swinging lever arm also helped to explain why substantial changes in the cross-bridge orientation were difficult to see: Only a small fraction of the cross-bridge mass moves much during the power stroke. Furthermore, it gradually became clear that the proportion of cross-bridges taking part in a contraction at any one time was only a small fraction of the total (see e.g. 24), which makes the registration of active cross-bridge movement doubly difficult.

STRUCTURES OF ACTIN AND MYOSIN

Atomic Structure of Actin

Thin filaments (f-actin) are helical polymers which have 13 actin molecules (42 kDa) arranged on six left-handed turns repeating every 36 nm. The rise per subunit is 2.75 nm. The morphology of the actin helix is, rather, two intertwined, steep right-handed helices. Along each of the morphological helices the actin monomers are spaced by 5.5 nm. The structure of the monomer (g-actin) was solved by protein crystallography as a complex with DNase I (25) and has since been solved in two other complexes (26, 27). The structure shows actin to consist of two similar domains each of which contains a 5-stranded β-sheet and associated α-helices. The phosphate moiety of a nucleotide (ATP or ADP), together with Mg^{2+} or Ca^{2+} (Mg^{2+} is physiological), is bound between the two β-sheet domains. Each of the domains carries a subdomain; one is involved in actin-actin interactions, and the other in addition forms the top of the nucleotide-binding pocket.

Orientated gels of filamentous actin yield X-ray fiber diagrams to about 0.6-nm resolution. Fiber diffraction patterns were calculated from models produced by placing the g-actin atomic structure in the helix for all possible orientations. A computer search compared the calculated and observed X-ray fiber diagram to find the best fit (28). The structure was refined to allow for the conformational changes taking place in actin on polymerization (29; Figure 3). The most notable movement is that the subdomains move 0.3- to 0.4-nm closer together in f-actin, closing off the ATP/ADP-binding site, which leads to a very low nucleotide exchange rate (after polymerization, the nucleotide in f-actin plays a structural rather than a metabolic role). A structure showing the reverse movement (i.e. an opening of the ADP/ATP-binding site), which may be essential for nucleotide

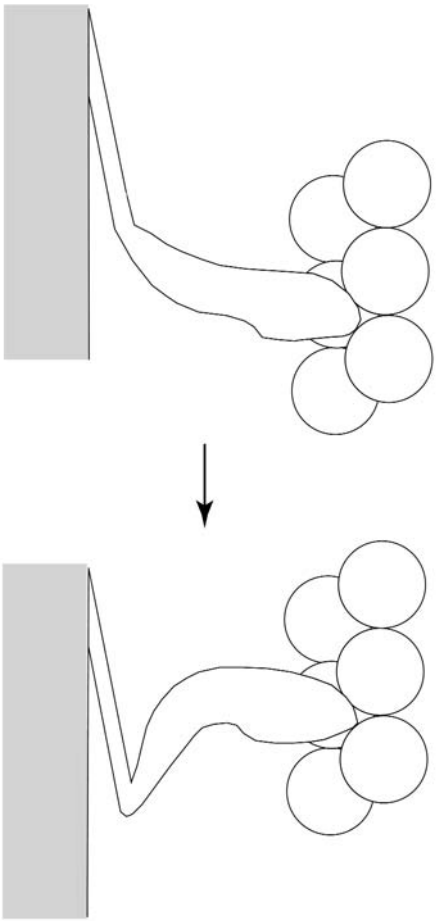

Figure 2 The major change in the cross-bridge is confined to the distal part, which moves as a lever arm (23).

exchange, has been reported (30). The contacts along the two long-pitch helices are substantial in area (>30 nm^2), in accord with the fact that the total pull on the filament (~1000 pN) is transmitted through this contact.

Atomic Structure of Myosin S1

In this section we refer to the chicken skeletal myosin sequence. Where ambiguity might occur, we preface the numbering with Sk. In later sections we also refer to *Dictyostelium* myosin by Dy and chicken smooth muscle by Sm (see Table 1).

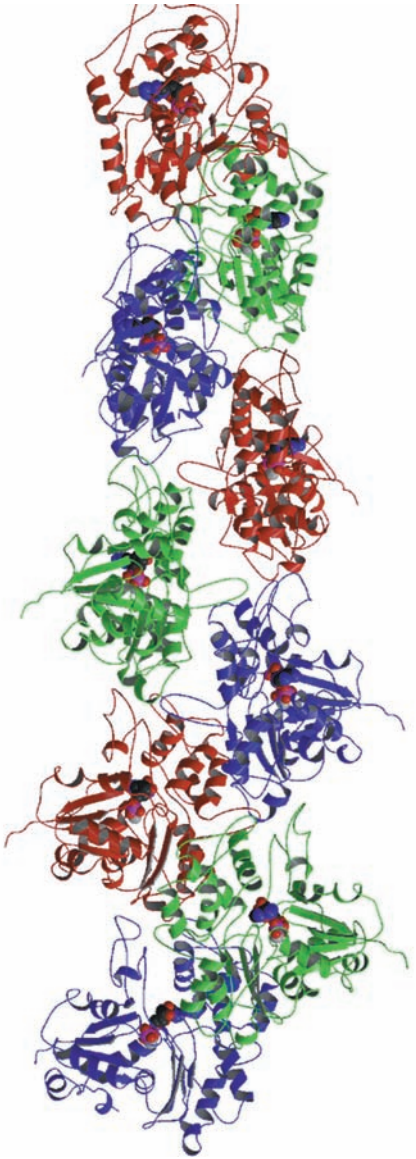

Figure 3 Structure of F-actin (28, 122). F-actin has 13 actin molecules arranged on six left-handed turns repeating every 36 nm. The rise per subunit is 2.75 nm. The morphology of the actin helix is two intertwined, long-pitch, right-handed helices. Along each of the morphological helices, the actin monomers are spaced by 5.5 nm. The structure of the monomer (g-actin) (25) shows actin to consist of two similar domains, each of which contains a five-stranded β-sheet and associated α-helices. [Figure prepared by using Bobscript and Raster3D (123, 124).]

TABLE 1 Sequence comparisons.

```
Sm   2  AQKPLSDDE KFLFVDKNFV NNPLA.QADW SAKKLVWVP. SEKH..GFEA ASIKEEKGDE
Sk   6  EMAAFGEAA PYLRZSEKER IEAQ..NZPF DAZSSVFVV. HPKE..SFVZ GTIQSZEGGZ
Dy   4  IHDRTSDYH KYLKVKQGDS DLFKLTVSDK RY...IWYNP DPDERDSYEC GEIVSETSDS

                          SH3 ←|
Sm  57 VTVELQENGK KVTLSKDDIQ KMNPPKFSKV EDMAELTCLN EASVLHNLRE RYFSGLIYTY
SK  60 VTVZTEG.GE TLTVKEDQVF SMNPPZYDZI EDMAMMTHLH EPAVLYNLZE RYAAWMIYTY
Dy  60 FTFKTVDGQD R.QVKKDDAN QRNPIKFDGV EDMSELSYLN EPAVFHNLRV RYNQDLIYTY

           c                                              c
Sm117 SGLFCVVINP YKQLPIYSEK IIDMYKGKKR HEMPPHIYAI ADTAYRSMLQ DREDQSILCT
Sk119 SGLFCVTVNP YZWLPVYNPZ VVLAYRGKKR QEAPPHIFSI SDNAYQFMLT DRENQSILIT
Dy119 SGLFLVAVNP FKRIPIYTQE MVDIFKGRRR NEVAPHIFAI SDVAYRSMLD DRQNQSLLIT

      P-loop                              Loop 1
      |     |
Sm177 GESGAGKTEN TKKVIQYLAV VASSHKGKKD TSITQGPSFS YGELEKQLLQ ANPILEAFGN
Sk179 GESGAGKTVN TZRVIQYFAT IAASGEKKKE EQSGKMQGT. ...LEDQIIS ANPLLEAFGN
Dy179 GESGAGKTEN TKKVIQYLAS VAGRNQANGS GVLEQQILQ. .......... ANPILEAFGN

               SW-I
                  *      c       c
Sm237 AKTVKNDNSS RFGKFIRINF DVTGYIVGAN IETYLLEKSR AIRQAKDERT FHIFYYLIAG
Sk235 AZTVRNDNSS RFGZFIRIHF GATGKLASAD IETYLLEZSR VTFQLPAERS YHIFYQIMSN
Dy228 AKTTRNNNSS RFGKFIEIQF NNAGFISGAS IQSYLLEKSR VVFQSETERN YHIFYQLLAG

Sm297 ASEQMRNDLL LEGFN NYTF LSNGHVPIPA QQDDEMFQET LEAMTIMGFT EEEQTSILRV
Sk295 ZZPELIDMLL ITTNPYDYHY VSEGEITVPS IDDQEELMAT DSAIDILGFS ADEZTAIYZL
Dy288 ATAEEKKALH LAGPESFNYL NQSGCVDIKG VSDEDEFKIT RQAMDIVGFS QEEQMSIFKI
```

```
                                                                    c
Sm356 VSSVLQLGNI VFKKERNTDQ ASMPDNTAAQ KVCHLMGINV TDFTRSILTP RIKVGRDVVQ
Sk355 TGAVMHYGNL KFZQZQREEQ AEPDGTEVAD ZAAYLMGLNS AELLKALCYP RVGVGNEAVT
Dy348 IAGILHLGNI KFEKGAGEGA VLKDKTALNA ASTVFGVNPS VLEKALME.P RILAGRDLVA

                                                          50kD Linker
                                  *    c                      $ *    $
Sm416 KAQTKEQADF AIEALAKAKF ERLFRWILTR VNKALDKTKR QGASFLGILD IAGFEIFEIN
Sk415 ZGETVSQVHN SVGALAZAVY EZMFLWMVIR INQQLD.TKQ PRQYFIGVLD IAGFEIFDFN
Dy407 QHLNVEKSSS SRDALVKALY GRLFLWLVKK INNVL..CSE RAAYFIGVLD ISGFEIFKVN

                     SWII-helix                        Loop
                   $                                §     c
Sm476 SFEQLCINYT NEKLQQLFNH TMFILEQEEY QREGIEWNFI DFGLDLQPCI ELIERPTNPP
Sk474 SFEQLCINFT NEZLQQFFNH HMFVLEQEEY ZZEGIEWEFI DFGMDLAACI ELIEZPM...
Dy465 SFEQLCINYT NEKLQQFFNH HMFKVEQEEY LKEKINWTFI DFGLDSQATI DLIDGRQ PP

                                                                   c
Sm536 GVLALLDEEC WFPKATDTSF VEKLIQEQGN HAK.FQKSKQ LKDKTE.FC. ILHYAGKVTY
Sk531 GIFSILEEEC MFPKATDTSF ZNZLYDEHLG KSNNFQKPKP AKGKAEAHFS LVHYAGTVDY
Dy523 GILALLDEQS VFPNATDNTL ITKLHSHFSK KNAKYEE..P RFSKTEFGV. .THYAGQVMY

                                                  Loop 2
          *              c
Sm593 NASAWLTKNM DPLNDNVTSL LNQSSDKFVA DLWKDVDRIV GLDQMAKMTE SSLPSASKTK
Sk591 NISGWLEZNZ DPLNETVIGL YQZSSVZTLA LLFATYGGEA EGGGGKKGGK KKGSS.....
Dy580 EIQDWLEKNK DPLQQDLELC FKDSSDNVVT KLFNDPNIAS RAKKGAN... ..........
```

continued

TABLE 1 *continued*

```
                Fig 6a helix                                                SH2
                                                                             |  #
Sm653 KGMFRTVGQL YKEQLTKLMT TLRNTNPNFV RCIIPNHEKR AGKLDAHLVL EQLRCNGVLE
Sk646 ...FQTVSAL FRENLNZLMA NLRSTHPHFV RCIIPNETZT PGAMEHELVL HQLRCNGVLE
Dy627 ...FITVAAQ YKEQLASLMA TLETTNPHFV RCIIPNNKQL PAKLEDKVVL DQLRCNGVLE

       SH1                          Converter Domain
      #   |  # |→    c   c
Sm713 GIRICRQGFP NRIVFQEFRQ RYEILAANAI PKG.FMDGKQ ACILMIKALE LDPNLYRIGQ
Sk703 GIRICRKGFP SRVLYADFKQ RYRVLNASAI PEGQFMDSKQ ASEKLLGGGD VDHTQYAFGH
Dy684 GIRITRKGFP NRIIYADFVK RY.YLLAPNV PRD.AEDSQK ATD.VLKHLN IDPEQYRFGI

                                 Essential LC
                        ←||→                          ←|→
Sm772 SKIFFRTGVL AHLEEERDLK ITDVIIAFQA QCRGYLARKA FAKRQQQLTA MKVIQRNCAA
Sk763 TZVFFZAGLL GLLEEMRDDZ LAEIITRTQA RCRGFLMRVE YRRMVERRES IFCIQYNVRS
Dy742 TKIFFRAGQL ARIEEAREQR ISEIIKAIQA ATRGWIARKV YKQAREHTVA ARIIQQNLRA

Regulatory LC
               * *
Sm832 YLKLRNWQWW RLFTKVKPLL Q
Sk823 FMNVZHWPWM ZLFFZIKPLL K
Dy802 YIDFKSWPWW KLFSKARPLL K
```

Comparison of the myosin head sequences for the chicken skeletal (Sk), Chicken smooth (Sm) and the *Dictyostelium* cytoplasmic myosin II (Dy). The residue number for the first residue in each line is given. The parts of the molecule discussed in the text are highlighted in color and/or labeled above.

KEY

Color codes for residues

W	Tryptophans, * above the residue indicates it is conserved in all 3 myosins, § above indicates the important Trp 510
C	SH1 and SH2 essential thiols
blue	Point mutations in *Dictyostelium* or smooth muscle MII $ is above the non-hydrolyser mutations # is above the Glycines in the essential SH/hinge region
blue underlined	Termination sites for crystallized proteins Dy 754 and 759, Sm 790 and 819
cyan	P-loop, helix shown in Fig 6a, Loop following SWII, link between upper and lower 50kD domain, Loop following Sk-W510
red	Loop 1, Loop 2 and converter domain
magenta	SWI and SWII loops
c	above the residue indicates a Cardiomyopathy point mutations.
* *	above the Sk-R245 and Sk-E468 indicates the salt bridge.

The proteolytic fragment S1 comprises the first 843 residues of the heavy chain together with the two light chains. It is the morphological cross-bridge and contains all the enzymatic activity of myosin (31, 32). Further limited proteolysis breaks the S1 into three fragments named after their apparent molecular masses—25K (N terminal), 50K (middle), and 20K (C terminal) (33). These fragments were thought to represent subdomains of the S1. The structure of S1 (see below) shows them rather to mark the positions of flexible loops (loop 1 and loop 2) in the S1 (for a discussion of the function of the loops, see below; see also 14).

The first X-ray crystal structure (34) was of S1 from chicken muscle without nucleotide but with a sulfate ion in place of the β-phosphate in the active site. The structure shows the S1 to be tadpolelike in form (Figure 4), with an elongated head consisting of a 7-stranded β-sheet and a C-terminal tail. All three fragments (25K, 50K, and 20K) contribute to the 7-stranded β-sheet. Numerous α-helices that surround the β-sheet form a deep cleft extending from the nucleotide-binding site to the actin-binding site. The C-terminal tail, which in the intact myosin molecule is connected to the thick filament, forms an extended α-helix that binds the two calmodulin-like "light chains." In Figure 4, the proteolytic fragments are color coded as follows: 25K (N terminal), green; 50K, red; and 20K (C terminal), blue. The 50K fragment actually spans two domains, which Rayment et al (34) have called the 50K upper domain and the 50K lower domain or actin-binding domain. The actin-binding domain has been colored *grey*. The N terminus lies near the start of the tail, and the first 80 residues form a protruding SH3-like β-barrel domain of unknown function [not present in all myosins (3)]. The rest of the 25K fragment, together with the 50K upper fragment (residues 81–486) form one large domain that accounts for 6 of the 7 strands of the β-sheet and constitutes the bulk of the molecule. The ATP-binding site is in this large domain near the 25K–50K fragment boundary and contains a characteristic P-loop similar to that found in some other ATPases and G-proteins (18). The ATP-binding site is about 4.0 nm from the actin-binding site. The 50K lower fragment (nucleotides 487–600) actually forms a well-defined domain that constitutes the major part the actin-binding site. A large, positively charged disordered loop (625–647) follows, which is also involved in actin binding. The first part of the ensuing 20K domain (648–689) is an integral part of the 25K–50K domain and consists of a long helix running from the actin-binding site to a seventh strand of the β-sheet. This is followed by a turn and a broken helix containing two reactive thiols (SH1707 and SH2697). Comparison with other structures (see below) shows that the end of the SH1 helix forms the hinge for the ensuing lever. There follows a small compact domain (711–781) which has been termed the "converter" domain (35, 35a). This functions as a socket for the C-terminal α-helical tail, which has been called the regulatory domain or "neck" and which carries the two light chains. The main function of the neck, however, appears to be as a lever arm to amplify rotational movements experienced by the converter domain during ATP hydrolysis (see discussion below).

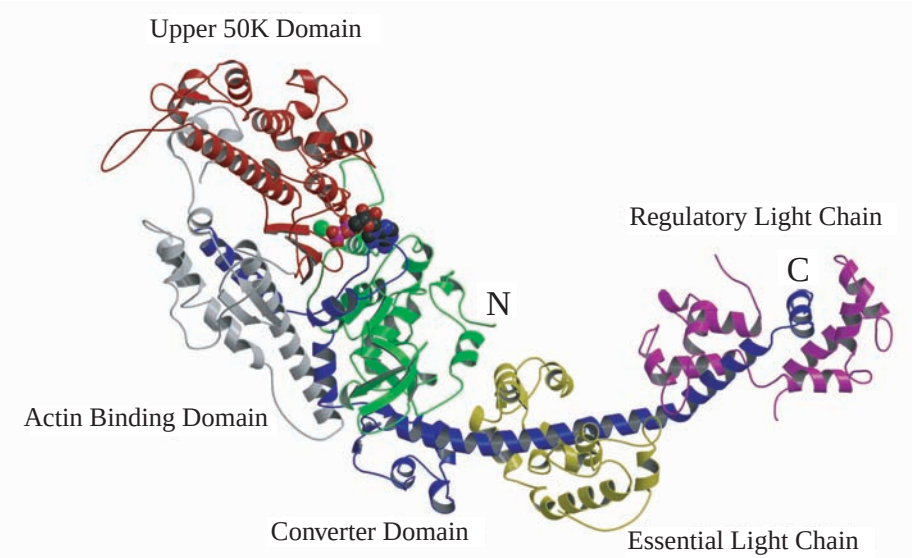

Figure 4 Myosin S1 (34). Myosin S1 has an elongated head consisting of a seven-stranded β-sheet and a C-terminal tail or "neck" which carries two calmodulin-like light chains—the regulatory light chain (*magenta*) and the essential light chain (*yellow*). The proteolytic fragments are color coded as follows: 25K (N terminal), *green*; 50K, *red*; and 20K (C terminal), *blue*. The 50K fragment spans two domains: the 50K upper domain and the 50K lower domain or actin-binding domain. The actin-binding domain has been colored *grey*. All three fragments (25K, 50K, and 20K) contribute to the seven-stranded β-sheet. Numerous α-helices that surround the β-sheet form a deep cleft extending to the actin-binding site. [Figure prepared by using Bobscript and Raster3D (123, 124).]

Actomyosin

An atomic model of the actin myosin complex (Figure 5; 36, 37) was obtained by fitting the atomic structures of f-actin and S1 into three-dimensional cryo-electron microscope reconstructions of "decorated actin." Decorated actin is produced by incubating f-actin with S1 in the absence of nucleotides. One cross-bridge (S1) binds to each actin monomer. Decorated actin is taken as a model of the rigor complex between actin and myosin. The atomic model of chicken muscle S1 was without nucleotide and therefore was thought to be close to the rigor configuration. This view may need some modification. The S1 binds to the lower side of one domain of actin but with a considerable contact to the subdomain of the next actin molecule below. The actin-binding sites and nucleotide-binding sites are on opposite sides of the sheet and are separated by 4–5 nm. The cleft in myosin extends from the ATP-binding site to the actin-binding site so that movements in this cleft could provide a physical link

between the ATP site and the actin-binding site. The very extended C-terminal α-helix of S1 lies distal to the actin helix and is ideally situated and orientated to function as a lever arm.

Truncated S1—a Minimal Motor

Genetic manipulation is not only an essential tool for analyzing function but is also a powerful adjunct to structural studies, because it allows the production of well-defined units or subdomains. Unfortunately, the expression of myosin is restricted to eukaryotic hosts because it cannot be successfully expressed in prokaryotes. Two expression systems have been used: *Dictyostelium discoideum* (cellular slime mold), using a plasmid to express myosin II constructs in cells deficient in myosin II, and SF9 insect cells (*Spodoptera frugperda*), using baculovirus as a vector to express chicken gizzard (smooth-muscle) myosin.

Expression makes it possible to design a minimal model of the myosin motor by truncating the polypeptide chain. The truncations used mostly eliminate the neck and the associated light chains but leave the converter domain intact. The neck makes the myosin head very asymmetric: "Neckless" myosin heads are more globular and easier to crystallize. The expressed fragments correspond more or less with the myosin core, which has been identified by sequence comparisons to be common to all myosins—many myosins have quite different necks to skeletal muscle myosin, but all have very similar cores (3). Proteolytic cleavage of chicken myosin close to the core boundary produces a kinetically normal "motor" (38), whereas experiments with shorter constructs of expressed *Dictyostelium* myosin II S1 show that damage to the converter domain leads to S1 constructs with modified ATPases. However, the form truncated at Dy759 appears kinetically normal (39). Rayment and co-workers (40–42) initially studied a crystalline truncated fragment of *Dictyostelium* myosin II S1. More recently, studies from Carolyn Cohen's laboratory, of truncated chicken smooth-muscle constructs, have yielded a wealth of new structural data (see below) (47).

Crystallography of Truncated S1 Shows Two Conformations: OPEN and CLOSED

The crystal structures of the *Dictyostelium* myosin truncated at Dy759 (i.e. without the neck or lever-arm) have been determined with a number of ATP analogs, particularly ADP.BeF_x, ADP.AlF_4 (40), and ADP.vanadate (41) (because the coordination geometry of the vanadate ion is bipyramidal, ADP.vanadate complexes are used as analogs of the transition state, and BeF_3 is close to tetrahedral so that ADP.BeF_3 is expected to be an analog of the ATP state). Although the ADP.BeF_3 state looks similar to chicken muscle without nucleotides, as do complexes with ADP and other ATP analogs (42), the ADP.vanadate structure shows large changes in the S1 structure. These changes are also apparent with ADP.

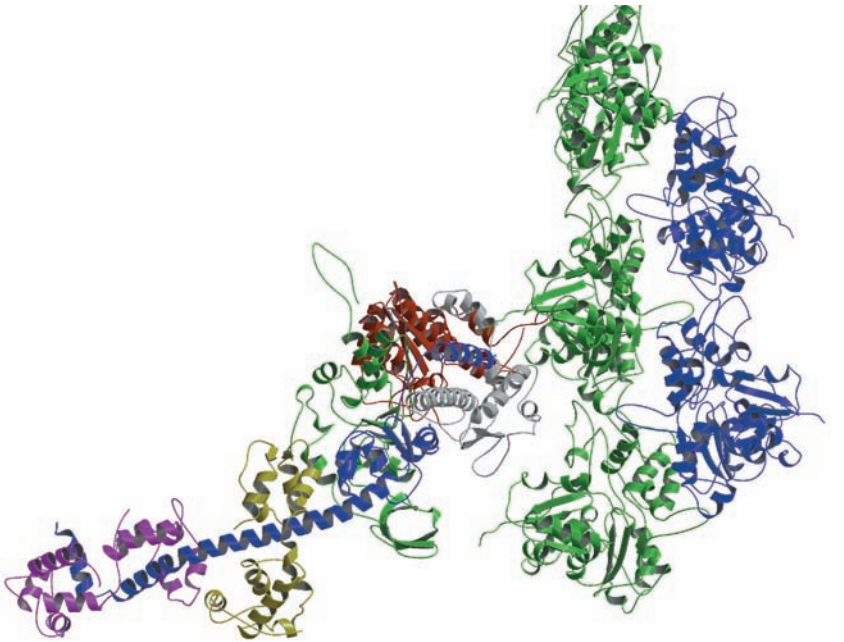

Figure 5 The structure of the acto-myosin complex (36, 37) shown are (*right*) five actin molecules in an actin helix and (*left*) a myosin cross-bridge (S1). Note that the cross-bridge makes contact with two adjacent actin monomers. [Figure prepared by using Bobscript and Raster3D (123, 124).]

AlF_4. The γ-phosphate–binding pocket closes, causing a partial closing of the 50K upper/lower-domain cleft, and there are large movements in the C-terminal region. The 50K upper domain and the actin-binding domain rotate a few degrees toward each other with the helix Sk648–666 as a fulcrum in a way that closes the nucleotide-binding pocket (Figure 6)—a movement of some 0.5 nm. At the same time the outer end of the long helix (residues Sk475–509, which, by analogy with the G-proteins, are called the switch-2 helix) and its associated loop (Sk509–519) bend out 24°. The switch-2 loop suffers extensive reorganization. We refer to this as the CLOSED form.

Switch 2 Should Close to Enable ATP-Hydrolysis

Smith & Rayment (41) note the similarity of the active site of CLOSED myosin with those of *Ras* p21 and other G-proteins. The differences between the OPEN and CLOSED forms in the neighborhood of the active site reside almost entirely in the conformation of the linker region (Sk465–470), which joins the 50K upper and lower domains. The authors point out that this region is

structurally equivalent to the switch-2 region in the protein product *Ras* p21, with which it also has a very strong sequence homology. The mutual rotation and closing of the 50k upper/lower-domain cleft causes movements of about 0.5 nm around the γ-phosphate–binding pocket. In the chicken crystal structure (OPEN form), which has no bound nucleotide (but with a bound sulfate in the γ-phosphate position) and which may be close to the end-of-power-stroke conformation, the switch-2 region is not part of the nucleotide-binding pocket. A similar movement of the switch-2 region that depends on trinucleotide being bound is also found in the G-proteins (43). A similar but even larger movement of the switch-2 region is found in the empty site of F1-ATPase, compared with the ATP or ADP sites (44). Only in CLOSED (e.g. in S1.ADP.vanadate) can the hydrogen bond (invariant for G-proteins, kinesins, and myosin but not present in F1 ATPase) between the amide of SkG466 and the γ-phosphate be formed. Moreover, in CLOSED the γ-phosphate is also coordinated by the Mg^{2+} ion, the invariant P-loop lysine, and S181 (45). Furthermore, through the formation of a salt bridge with SkR236, SkE468 comes close enough to the putative attacking water to stabilize and polarize this molecule. In OPEN, SkE468 takes on a different orientation. It is difficult to see how hydrolysis can proceed in OPEN, which would therefore appear not to be an Mg.ATPase: The closing would appear to be essential for enabling hydrolysis. Smith & Rayment (41) proposed that the CLOSED form is brought about by the formation of the transition state complex with the γ-phosphate stabilized in the pentacovalent intermediate conformation. However, ADP.BeF_3 complexes can also produce this state (see below).

ADP.BeF_3, an ATP Analog, Can Produce Both OPEN and CLOSED States

ADP.BeF_3 is thought to be an analog for ATP. Fisher et al (40) solved the structure of *Dictyostelium* S1 with ADP.BeF_3 bound in the active site and found it to be remarkably similar to skeletal chicken S1 without nucleotides. This result appears to show that the structure of the ATP state is OPEN, which is puzzling because it would not be able to hydrolyze the ATP. Moreover, the attitude of the converter domain (and hence inferred position of the neck or lever arm) is near to what we anticipate should be the end of the power stroke, which is also unexpected for the ATP state. More recently investigators (I Schlichting, A Becker, D Manstein & KC Holmes, manuscript in preparation) have solved the structure of an ADP.BeF_3 complex of truncated *Dictyostelium* S1 and found it to be essentially identical to the ADP.vanadate complex. The γ-phosphate–binding site is CLOSED, and the converter domain is in the rotated configuration. The construct used in this case was 5 residues shorter than that used by Fisher et al (40). This results in a tighter binding of ADP (46). It may be that the difference in binding energy of ADP.BeF_3 is adequate to favor the CLOSED structure: The transition between the two forms of myosin therefore appears to be sensitively poised.

Crystallographic studies on truncated forms of smooth-muscle myosin (47; see below) show the closed conformation with both ADP.BeF_3 and ADP.vanadate, so that it seems rather clear that the CLOSED form can accommodate ATP both in its normal and pentacovalent forms. It therefore seems reasonable to assume that the CLOSED form can also accommodate ADP.P_i without further substantial alterations of the protein conformation.

The Switch-2 Region Should Open for Phosphate Release

The CLOSED structure appears to generate a tight coordination pattern for the oxygens of the γ-phosphate both before and after cleavage, which would explain the high phosphate affinity. This interaction in turn is important for stabilizing the closed form when γ-phosphate is present. Opening the switch-2 region destroys the γ-phosphate–binding pocket and the SkE468–R245 salt bridge. These changes would appear to facilitate γ-phosphate release [a "back door enzyme" (48, 49)]. It seems very likely that actin binding favors the OPEN form and thereby facilitates phosphate release. Unfortunately, the structural basis of this important mechanism has yet to be revealed.

The Lever Arm

The movement of switch 2 in the CLOSED form has other more far-ranging consequences, namely the rotation of the converter domain through about 60°. Holmes (8, 50) used the coordinates of the chicken structure to provide the missing lever arm and proposed that the new orientation of the lever arm was indeed the beginning of the power stroke. A model of this new state is shown in Figure 7 (cf Figure 8). We show the corresponding diagram for the open state [truncated S1 with ADP.BeF_3 bound in the active site (40)], which may mimic an ADP state [i.e. the state after release of the γ-phosphate; cf the structure of chicken skeletal myosin with no nucleotide bound (Figure 6)]. The end of the lever arm has moved through 11 nm along the actin helix axis between OPEN and CLOSED, which is about the expected magnitude of the power stroke. This large change is driven through molecular cogs and gears by a small (0.5-nm) change in the active site. Therefore, it now seems rather likely that the myosin power stroke works by switching between these two conformations.

Smith & Rayment (41) were cautious of this interpretation because they thought that the truncation of the light chains might cause artifacts and also because the converter domain was apparently rather mobile. Moreover, the changes did not explain the chemical cross-linking effects (51). The subsequent structure of truncated *Dictyostelium* myosin with ADP.BeF_3 showed the converter domain in the second orientation very clearly (I Schlichting, A Becker, D Manstein & KC Holmes, manuscript in preparation), but still doubts about the integrity of such truncated constructs remained. Such doubts have been allayed by the publication of the structure of smooth-muscle myosin from Carolyn Cohen's laboratory.

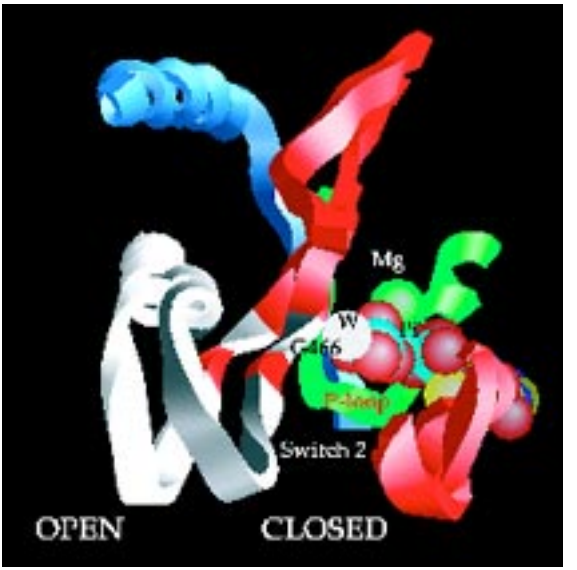

Figure 6a A view of the ATP-binding site looking out from the actin helix. Shown are the P-loop (*green*), an Mg.ATP molecule with the base at the back and the three phosphate groups in the front (carbon, *yellow*; nitrogen, *blue*; phosphate, *light blue*; oxygen, *red*; magnesium, *green*); parts of the 50K upper domain (*red*) including the so-called "switch-1" region (*right*); the switch-2 element in the open "ADP" (*white*) and closed "ATP" (*gray*) conformations—the conserved glycine (Sk466) is shown in *gray* or *white* (note that this residue moves about 0.5 nm between the two conformations); and the helix (Sk648–666), which acts as fulcrum for the relative rotation of the 50K upper and lower domains (*blue*).

Smooth-Muscle Myosin

Chicken smooth-muscle myosin truncated at Sm791 and Sm820 has been expressed in insect cells by using the baculovirus vector. The shorter construct stops at the end of the motor domain "core" (3) and the longer construct encompasses the essential light-chain binding site, that is, the first half of the lever arm, and is complete with the essential light chain. The structures of both constructs have been solved as complexes with ADP.vanadate and ADP.BeF_3 (47). All show the myosin cross-bridge in the CLOSED form (the putative pre-power-stroke orientation) with the converter domain in the rotated position essentially identical to that obtained in the two *Dictyostelium* constructs discussed above. There are no substantial differences arising from ADP.AlF_4 as compared with ADP.BeF_3, apparently showing that the nature of the ligand (ATP analog or transition state analog) does not control the protein conformation. Since all the smooth-muscle crystals display extensive noncrystallographic symmetry, CLOSED has now been obtained 16 times in a large variety of different environments. It seems, there-

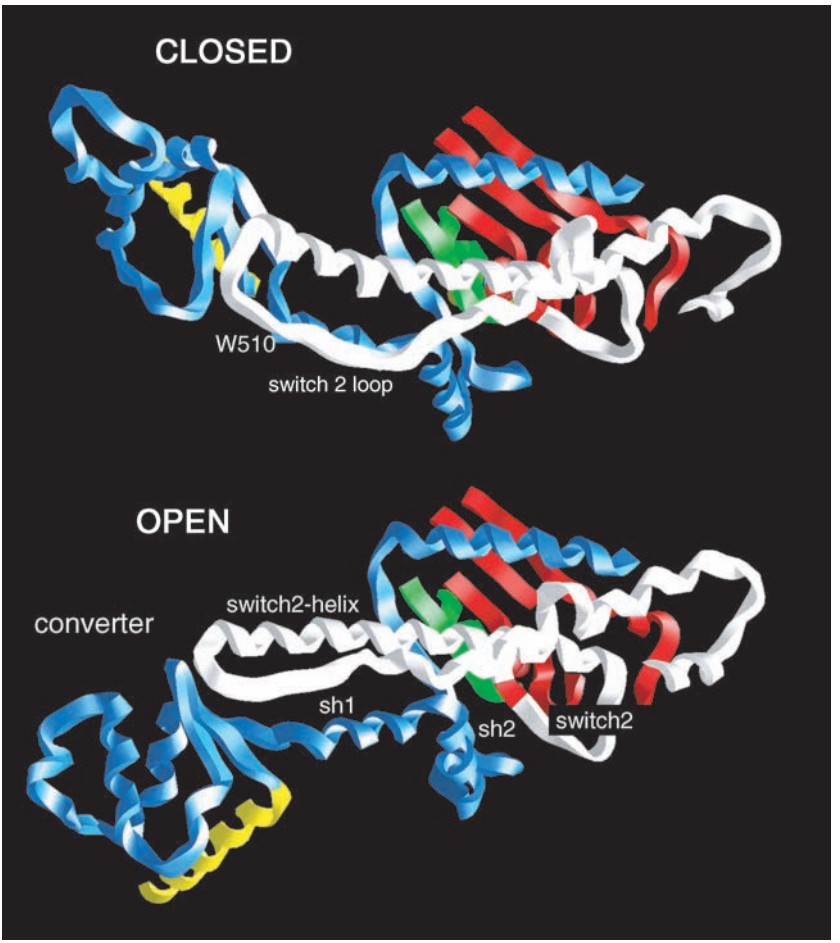

Figure 6b A view at right angles to the above with CLOSED at the top and OPEN below, showing the large changes in the orientation of the converter domain (*left*) resulting from the inward movement of the switch-2 element (*right*), which results in a bending and twisting of the switch-2 helix and the associated switch-2 loop, which carries the highly conserved W510. [Figures produced by using GRASP (125) from data sets described in the text.]

fore, that one can rule out the possibility that the CLOSED form is an artifact of truncation or crystalization.

An unexpected new insight into a possible control mechanism is provided by the essential light-chain construct (Figure 9). Here the converter domain is in the CLOSED (i.e. rotated) orientation, which leads to the lever arm helix starting out in the predicted manner. However at residue Sm792 there is a break in the helix so that the ensuing helix heads off at an angle about 8° inclined to the initial helix

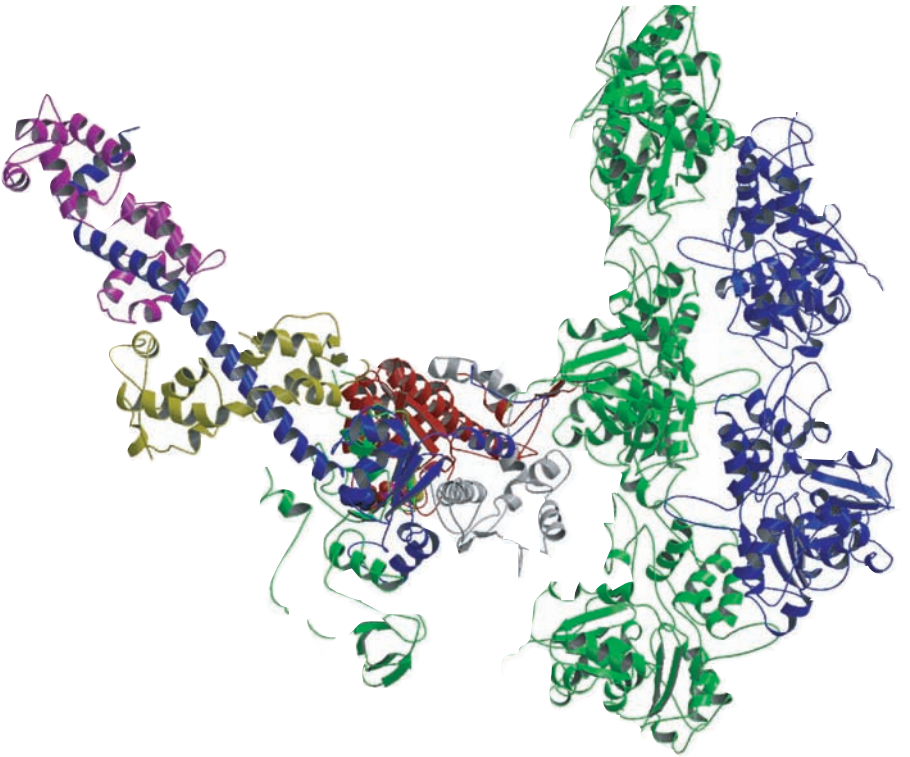

Figure 7 A reconstruction of the "pre-power-stroke" state from the crystallographic data on the *Dictyostelium* construct truncated at 759 and complexed with ADP.vanadate (41). Note the 70° rotation of the converter domain. The missing "neck" or lever arm has been modeled from chicken S1 data by superimposing the converter domains. To establish the orientation in relation to the actin helix (*right*), the 50K upper and lower domains have been superimposed on the corresponding domains in the chicken structure shown in Figure 5. Note the rotation of the converter domain compared with that in Figure 5. [Figure prepared by using Bobscript and Raster3D (123, 124).]

direction. This break is caused by the essential light chain forming a bond with the top of the 25K domain rather close to the 25K–50K junction (loop 1). The position of the lever arm inferred from this structure is very strongly angled to the muscle filament axis. It is possibly a parking position brought about by a regulatory function of the light chains.

Molecular Cogs and Gears

The smooth-muscle structures provide a wealth of new data. Moreover, now the complete coordinates of the moving parts are available for almost identical

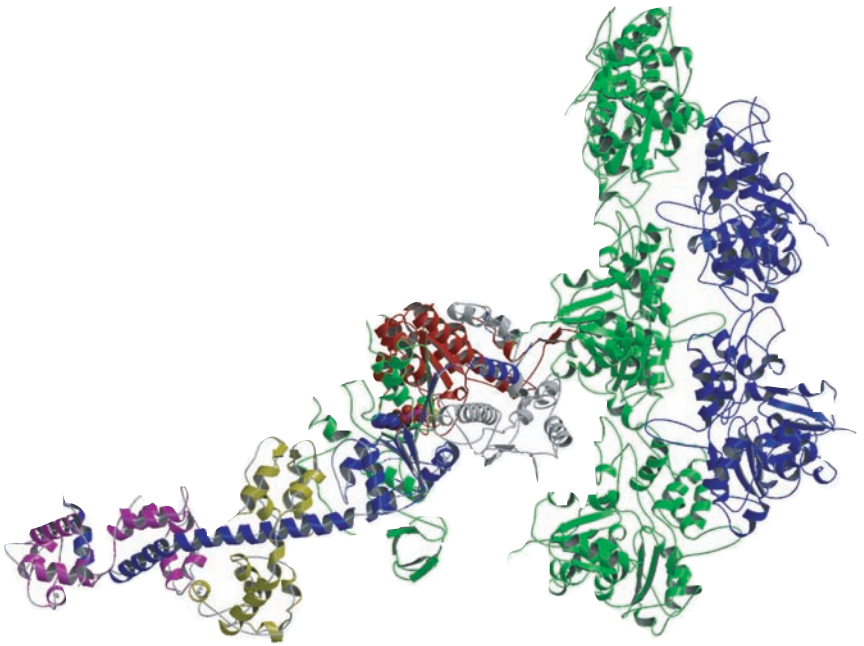

Figure 8 The "post-power-stroke" state: modeled from the crystallographic data on the *Dictyostelium* myosin motor domain truncated at residue 759 and complexed with ADP.BeF_3 (40). Details are as in Figure 7. The end of the lever arm moves about 11 nm between the two states. [Figure prepared with Bobscript and Raster3D (123, 124).]

sequences in both the OPEN (34; Brookhaven Protein Data Bank accession number 2MYS—chicken skeletal muscle with sulfate in the active site) and the CLOSED form (47; Brookhaven Protein Data Bank accession numbers 1BR1, 1BR2, and 1BR4—chicken smooth muscle with ADP.BeF_3 and ADP.AlF_4 in the active site). This allows a rather detailed analysis of the conformational changes between the OPEN and CLOSED forms, which are limited to the regions Sk460–520 (switch 2 and switch-2 helix) and the SH2-SH1 hinge (Sk694–716). Nearly all the changes take place by rigid-body rotations of secondary and tertiary structure elements. The basic movement that closes the γ-phosphate–binding site is a rotation of the actin-binding domain in relation to the 50K upper domain about the helix Sk648–666. This forces the SH1 helix against the switch-2 helix, which bends out at residue Sk497. As this happens the end of the switch-2 helix twists through about 60° (Figure 6*b*). This in turn causes a rotation of the converter domain (Sk711–781) with which the end of the switch-2 helix interacts by a strong hydrophobic bond. The fulcrum for the converter domain is provided by residues at the distal end of the SH1 helix (Sk707–711), each of which undergoes rather moderate changes in its ϕ, ψ

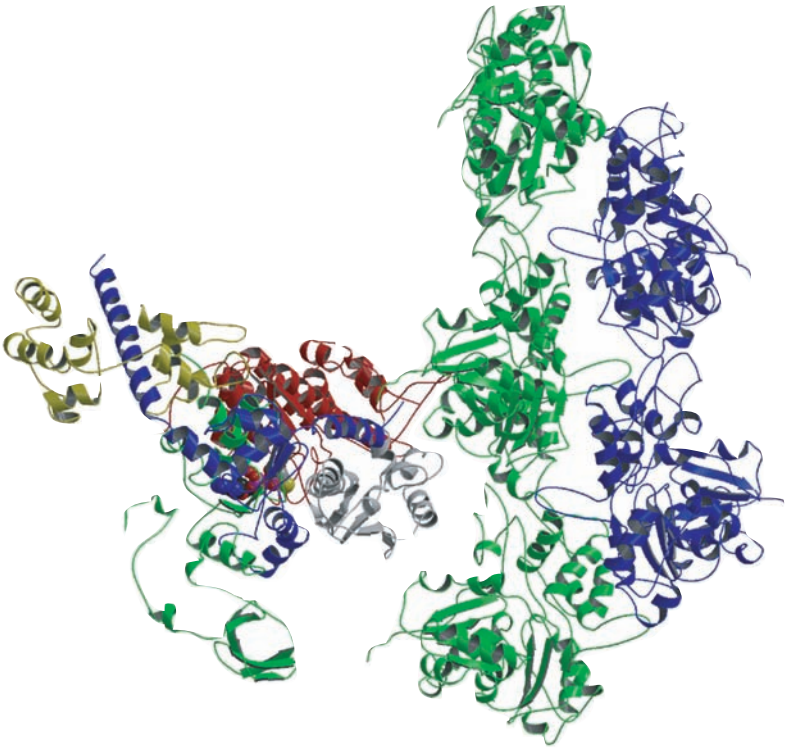

Figure 9 Structure of smooth-muscle myosin truncated at 819, carrying the essential light chain and with ADP.AlF_4 or ADP.BeF_3 bound in the active site (47). The molecule has been orientated in relation to the actin helix by superimposing the 50K domain with the 50K domain of chicken S1. Note the similarity to Figure 7. The structure is CLOSED (i.e. pre-power-stroke), and the converter domain is in the rotated position. There is a break in the lever arm helix at residue Sm792; the ensuing helix heads off at an angle of about 8° to the initial helix direction. The essential light chain contacts the top of the 25K domain rather close to Loop 1. [Figure prepared by using Bobscript and Raster3D (123, 124).]

angles. The angle between the SH1 helix and the SH2 helix alters by a rotation that mostly occurs at SkG699. There is no evidence of a melting or disordering of the SH1–SH2 helices, as has been suggested by chemical cross-linking experiments (51). In fact the SH2 helix hardly moves. The physiological significance of the cross-linking experiments remains to be explained.

This comparison shows up a remarkable fact: The transition from OPEN to CLOSED is achieved by substantial movements in only a very few residues (Table 2). The largest ϕ, ψ changes are limited to the switch-2 loop (i.e. residues Sk509–519), which includes the invariant W510 (the side chain moves from a solvent exposed environment to a shielded environment) and the following highly

conserved sequence EFIDFGM where, in particular, G516 suffers a peptide flip. In the *Dictyostelium* OPEN form, which we equate with the ADP form (see below), the switch-2 loop is in fact disordered.

At this preliminary level of analysis the changes are not reminiscent of a state change (e.g. the R-T transformation of hemoglobin, with helices clicking from one position to another with a high activation energy) but rather appear like the meshing of cogs and gears. Apart from changes in the γ-phosphate–binding pocket itself, which includes the formation of a salt bridge, it appears that the transformation might occur without an appreciable activation energy. The myosin structure might be able to flop easily between the two states to take up any intermediate state (52) in response to external forces (such as the effects of actin binding and tension on the molecule). This would be a very desirable property for a molecular machine.

OTHER EVIDENCE FOR A SWINGING LEVER ARM

Effects of ADP on the Structure of Decorated Actin

The ideal experiment for observing the power stroke (i.e. the transition from OPEN to CLOSED while bound to actin) would be to add ATP to decorated actin and observe the change in the myosin cross-bridge orientation by electron microscopy. This experiment is difficult to perform since the ATP causes rapid dissociation of the actin-myosin complex. Two experiments using time-resolved methods (53, 54) have produced apparently inconsistent answers. A more robust approach is to look for the effects of adding ADP, which does not lower the actin-myosin affinity enough to cause dissociation in an electron microscope experiment. Although with skeletal muscle S1 there is no observable effect on binding ADP, for smooth muscle and some other myosins the addition of ADP to decorated actin caused quite large changes in the angle of the lever arm (55, 56), which can be clearly observed by cryoelectron microscopy. This effect seems to be limited to actomyosins with a relatively high affinity for ADP. Although clearly this is not an effect that can be related to phosphate release, these experiments are noteworthy for providing the first incontrovertible evidence of lever arm movement in response to nucleotide binding.

Use of Fluorescent Probes to Measure Lever Movement

Fluorescence polarization measurements provide a convenient method of measuring lever arm orientation if the probes can be attached in a way that hinders probe rotation and does not inhibit myosin function. Because the atomic structures of the light chains are known (34, 35), genetically engineered light chains can be manufactured with SH groups in suitable positions to allow difunctional chromophores to be securely attached. Furthermore, the chemically modified light chains can be diffused into muscle fiber and exchanged for endogenous light chains. This approach has been used by Goldman and collaborators to show

TABLE 2 ϕ ψ Values

OPEN			CLOSED		
Sk	ϕ	ψ	ϕ	ψ	**Sm**
M495	−77.0	−32.0	−88.4	−43.1	M497
Z496	−73.3	−40.7	−114.8	−52.2	F498
V497	−61.2	−50.6	−55.9	−70.6	I499
L498	−56.8	−54.6	−50.5	−55.0	L500
E499	−48.6	−60.6	−49.7	−45.4	E501
Z500	−50.4	−18.6	−72.3	−27.2	Q502
E501	−77.0	−41.5	−59.7	−50.3	E503
E502	−59.0	−60.6	−60.8	−29.2	E504
Y503	−52.5	−12.5	−64.9	−41.3	Y505
Z504	−92.7	−38.6	−64.6	−59.6	Q506
Z505	−66.3	−52.0	−40.6	−63.5	R507
E506	−71.5	−45.4	−61.8	−17.5	E508
G507	111.0	16.5	68.0	50.6	G509
I508	−77.1	160.2	−90.9	160.7	I510
E509	−113.2	85.9	−65.7	91.9	E511
W510	−126.1	122.0	−150.6	141.4	W512
E511	−109.8	138.6	−114.1	144.3	N513
F512	−160.4	149.2	−63.6	161.3	F514
I513	−79.1	147.3	−143.6	121.7	I515
D514	−47.4	138.0	−92.8	102.7	D516
F515	−83.6	−13.4	−78.5	−2.0	F517
G516	−63.2	−49.0	48.5	65.0	G518
M517	−32.3	−33.5	−140.9	89.3	L519
D518	−62.2	−27.8	−144.0	138.0	D520

continued

that in contracting muscle fibers the light chains swing through angles that are quite consistent with the molecular models for the swinging lever arm proposed above, if one assumes that only a small proportion of the cross-bridges are active at any one time (24, 57).

Making the Lever Arm Longer or Shorter

The length of the lever arm can be altered by inserting or deleting light-chain–binding sites (58, 59). Alternatively an artificial lever arm fabricated from α-actinin repeating units can be added to the myosin core (60). In both experiments modified-*Dictyostelium*–expressed myosin was used for in vitro motility

TABLE 2 *continued*

OPEN			CLOSED		
Sk	ϕ	ψ	ϕ	ψ	**Sm**
L519	−93.5	−15.8	−128.4	11.0	L521
A520	−49.6	−32.5	−44.2	−53.2	Q522
R696	−77.8	−42.9	−90.5	−57.0	R706
C697	−80.9	−10.4	−71.9	−9.2	C707
N698	−76.6	−46.3	−96.3	−15.6	N708
G699	118.3	−13.8	78.1	27.6	G709
V700	−57.4	−46.3	−56.7	−65.2	V710
L701	−76.3	−17.8	−44.0	−60.0	L711
E702	−88.5	−22.7	−54.2	−45.5	E712
G703	−78.3	−26.8	−52.8	−16.2	G713
I704	−74.6	−41.1	−104.3	−32.7	I714
R705	−53.8	−60.4	−51.8	−51.6	R715
I706	−56.1	−25.5	−61.8	−34.4	I716
C707	−75.2	−49.9	−62.9	−32.7	C717
R708	−68.0	8.3	91.3	−44.5	R718
K709	−104.2	−30.8	−64.5	−62.7	K719
G710	−89.1	−129.9	−84.5	−162.5	G720
F711	−119.7	88.5	−122.1	81.9	F721
P712	−49.3	−91.2	−64.2	2.1	P722
S713	−57.7	128.8	−125.9	134.1	S723
R714	−133.1	144.9	−143.4	151.2	R724
V715	−94.1	133.2	−151.9	135.6	V725
L716	−78.8	135.7	−72.4	140.8	L726

assays in which the speed of transport of actin filaments across a lawn of myosin heads was measured. It was shown that the ATPase rates of the constructs were unaffected by the alterations to the lever arm, in which case the speed of transport would be expected to be proportional to the length of the lever arm. In both cases it was found that the speed of actin transport was indeed proportional to the length of the lever arm. Moreover, in the experiments of Uyeda et al (59) an extrapolation could be made to the point of zero velocity. This came out with a radial position behind the converter domain very close to the SH1 hinge discussed above. In all these studies only the motility was measured; it will be of interest to determine whether the force produced also scales with the length of the lever arm.

MYOSIN S1 KINETICS

Allocation of States to Kinetic Schemes

The biochemical mechanism of ATP hydrolysis by myosin was defined in the 1970s and became known as the Bagshaw-Trentham scheme (61), and although there have been minor modifications, the scheme outlined below has remained largely unchanged. All myosins studied to date follow this same basic mechanism with modifications in both the overall ATPase rate and the relative rates of individual steps (62–65).

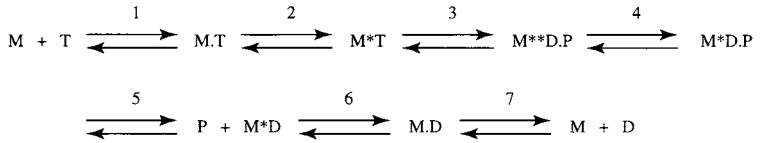

The best characterized myosin is the subfragment 1 from rabbit fast muscle. In this myosin ATP binds in a two-step process, a diffusion-limited reaction (step 1) followed by a fast almost irreversible conformational change, which results in an increase in the intrinsic protein fluorescence (step 2). Reversible ATP hydrolysis then occurs at a rate of >100 s^{-1} accompanied by a further increase in fluorescence with an equilibrium constant of ~10 (step 3). The products remain tightly bound to the protein and a slow (0.05 s^{-1}) protein isomerization is required (step 4) before P_i is rapidly released (step 5). A fluorescence decrease accompanies step 4. After P_i release, ADP dissociates in a two-step reaction that is essentially the reverse of steps 1 and 2 and is associated with a further fall in fluorescence.

In terms of the above scheme, the state OPEN would most simply be assigned to the M*N state because it is observed with crystals containing ADP, AMP.PNP, ATPγS (an unhydrolyzable ATP) bound to the nucleotide site. The fluorescence change accompanying nucleotide binding is most likely the result of a perturbation of SkW113 and or SkW131 in the nucleotide-binding pocket, because myosins lacking these tryptophan residues show little fluorescence change on nucleotide binding [e.g. *Dictyostelium* and Scallop (62, 66)].

The state CLOSED therefore would correspond to M**ADP.P_i or the transition state of the hydrolysis reaction. *Dictyostelium* and both chicken myosins show a fluorescence change accompanying the hydrolysis step. Of the three tryptophan residues in the motor domain common to *Dictyostelium* and chickens, the local environments of SkW440 (Dy432) and SkW595 (Dy584) do not alter appreciably between OPEN and CLOSED forms. Therefore they are not strong candidates for the intrinsic fluorescence signal. However SkW510 (Dy501) sits close to the junction between the switch-2 helix and the converter domain and twists from a solvent-exposed to solvent-shielded environment between OPEN and CLOSED. Therefore it is a priori a good candidate for the signal (see also 13 and 67). Thus the protein fluorescence change accompanying hydrolysis would arise from the perturbation of SkW510, which signals the movement of switch 2 and the lever

arm. However, as noted above, state OPEN appears to be noncompetent for hydrolysis. Thus the conformational change must precede hydrolysis. We therefore need to consider step 3 as comprising two events: Step 3a is the conformational change, and step 3b is the hydrolysis step. Unusual in this scheme is the notion that hydrolysis should be fast and not associated with a large protein isomerization. On the other hand, 3a is a very significant isomerization because the converter domain and lever arm move a large distance as the pocket shuts.

$$M^*ATP \underset{3a}{\rightleftharpoons} M^{**}ATP \underset{3b}{\rightleftharpoons} M^{**}ADP.Pi$$

In all measurements made to date the second component of the fluorescence change and the hydrolysis step occur at the same observed rate. Therefore, hydrolysis must very quickly follow the conformational change; otherwise a significant lag of the hydrolysis behind the fluorescence change would have been observed. The hydrolysis step is also readily reversible ($K_3 = 10$), that is, it occurs with a very small free-energy change and has fast forward and reverse rate constants ($k_{+3} + k_{-3}$ 100 s^{-1}) (68). The simplest assignment of the rate constants to the two components of step 3 is therefore that k_{+3a}100 $s^{-1}$and k_{-3b}10 $s^{-1}$with k_{+3b}, k_{-3a} >> 100 s^{-1}. Thus M**ATP is an unstable state, breaks down rapidly in either the forward or reverse direction, and as such has many characteristics of a transition state. This should not to be confused with the chemical transition state for the hydrolysis step, which is stabilized by the protein and may correspond to $M^{**}ADP.P_i$.

The small free-energy change for step 3 is known to be composed of large compensatory changes in enthalpy and entropy so that although there is only a small net change in ΔG, energy is being converted/stored in this step (69, 70).

The evidence for the fast rates of reversal of the hydrolysis reaction come largely from ^{18}O isotope exchange studies (71, 72), whereas the assignment of an equilibrium constant of 10 comes from analysis of the breakdown products on acid quenching the complex (68). The possibility that the $M^{**}ADP.P_i$ complex is a transition complex is not ruled out by these studies. Particularly the elegant work of Dale & Hackney (73) has demonstrated that, although the oxygens on the γ-P_i are rapidly exchanged with solvent, the position of oxygen isotopes on the β-P_i do not change. Thus it remains possible that the β-γ bond is not broken on forming $M^{**}ADP.P_i$ and that the γ-P_i is pentacovalent; that is, the attack by water has occurred but the ATP β-γP_i bond is not broken. Step 3 could therefore represent the formation of the pentacovalent γP_i complex (step 3b), which occurs concomitant with the OPEN to CLOSED conformational change (step 3a).

Sensitivity to γ-Phosphate

The OPEN form appears to be favored by initial ATP binding and by ADP; the CLOSED form is favored by ADP.vanadate and some other transition state analogs. One important difference between these forms appears to be the position of SkGly466 in switch 2, which corresponds to Gly60 in *ras* p21. In *ras* the

sensitivity of switch 2 to the presence of either GTP or GDP in the active site is a consequence of the coordination of the γ-phosphate of GTP by the amide nitrogen of G60. This coordination is also an important part of the hydrolytic machinery. In the OPEN form of myosin S1, this hydrogen bond cannot be made; in the presence of the γ-phosphate, the switch-2 region moves towards the binding pocket by about 0.5 nm to allow this H-bond to form. (see *Point Mutations of G466* below).

Note that in the switch-2 CLOSED form the phosphate is apparently coordinated by three strong bonds in addition to the covalent bond. There is no reason to believe it would rotate quickly after hydrolysis. The crystal structure therefore gives no indication of how the three γ-P_i oxygens can be rapidly exchanged with water oxygens.

The two crystal structures therefore are consistent with a major change in myosin conformation being associated with (or perhaps just before) the hydrolysis step and with this conformational change being largely a reversal (or a priming) of the conformational change of the power stroke driven by actin binding. This is essentially the scheme proposed by Lymn & Taylor (19) in 1971 and is the basis of Figure 1. At the time there was no direct evidence for this conformational change on the hydrolysis step, but it is a logical consequence of the mechanism they proposed.

To understand the complete ATPase cycle requires more detailed structural knowledge of the way in which actin reverses the CLOSED-OPEN conformational change.

Present Structures Do Not Illuminate the Mechanism of Actin-Induced ADP Release

Both OPEN and CLOSED have relatively high affinity for nucleotides, so that actin-mediated release of nucleotides must involve more structural change than we presently see. The effect of actin would not be expected to be simply a reversal of the OPEN-CLOSED change because one expects a vectorial mechanism to drive the cycle, which is provided by the requirement for P_i release to precede ADP release. The missing part of the cycle is the mechanism whereby actin binds to the CLOSED form and induces a series of conformational changes that lead to P_i release followed by ADP release. Whereas the transition CLOSED to OPEN would lead to P_i release, the structures give no indication of how actin induces ADP release and then ATP binding induces actin dissociation. Solution biochemical studies have provided several insights into the docking of actin with myosin and its effect on nucleotide binding to myosin.

THE ACTIN-MYOSIN INTERACTION

Kinetic Data

The current low-resolution structural view of actin binding to myosin suggests that no major rearrangement of the myosin takes place at the actin-myosin

interface but that large-scale changes occur on myosin distal to the actin-binding site. However this does not mean that no structural changes take place at the interface. In the interaction of any two proteins the docking is likely to involve initial diffusion-limited complex formation followed by a series of structural adjustments (induced fit) as the stereospecific interaction site is formed, along with induced conformational changes in the proteins. Kinetically the docking of myosin onto an actin filament can be resolved into at least three events (4). Initial complex formation, largely involving charge-charge interactions, is followed by two changes in conformation of the complex. The first may involve the formation of stereospecific hydrophobic interactions (4), and the second involves a major rearrangement of the actin-S1 complex because fluorescence probes on both actin and the nucleotide in the myosin pocket report the change simultaneously (74, 75). The second isomerization also appears to involve a large-volume increase of the complex, which is normally assigned to displacement of a large amount of water from the complex (76, 77).

$$A + M(N) \underset{}{\overset{K_0}{\rightleftharpoons}} \underset{\text{collision complex}}{A{\sim}M(N)} \overset{K_1}{\rightleftharpoons} \underset{\text{A-state}}{AM(N)} \overset{K_2}{\rightleftharpoons} \underset{\text{R-state}}{AM(N)}$$

The three events are best documented for rabbit myosin in the absence of nucleotide. As we apparently do not have a high-resolution structure of the nucleotide-free myosin S1, it is not simple to predict what actin binding will do to the S1 structure. However, the three events appear similar (but with marked changes in rate and equilibrium constants) for M.ADP (78, 79), and it is suggested that M.ADP.P_i binds in the same three steps, but the equilibrium constant for the last step is small (~1, weak binding to actin) until P_i is displaced from the myosin. The last of the conformational changes has been suggested to be closely coupled to the power stroke of the ATPase cycle (80–82).

The key feature of this mechanism is that the isomerization of step 2 results in a major strengthening of the actin binding to myosin and simultaneously a weakening of the nucleotide binding to actin. The equilibrium constant of this step varies for different nucleotides. Thus, in the absence of nucleotide, K_2 is large (>100), in the presence of ATP it is small ($K_2 << 1$), and ATP displaces actin. For other nucleotides and nucleotide analogs, K_2 is intermediate, and which form predominates, the ternary complex or the binary complex with either nucleotide or actin, depends on the concentrations used.

For fast rabbit myosin, the formation of the R-state reduces the affinity of the myosin head for ADP by more than 100-fold (79, 83), and the rate of ADP dissociation is accelerated more than 500-fold. These factors vary widely for different myosin types. For chicken smooth muscle myosin, for example, the ADP affinity is reduced only fivefold, whereas the dissociation rate is accelerated tenfold by actin (84). Actin also induces acceleration of P_i dissociation, typically more than 200-fold.

Correspondence with Structural Data

We can now address the question of the correspondence between the conformational changes detected by fluorescence probes in the kinetic measurements and the structures seen in the crystals. The current evidence suggests that the formation of the A-state (probably involving stereospecific interactions in the actomyosin interface) has little influence on the nucleotide-binding pocket, because the labels on the nucleotide do not detect formation of the A-state. Nor does the formation of the A-state significantly weaken the affinity of nucleotide for myosin. The formation of the A-state therefore appears to be limited to local changes at the actomyosin interface. Therefore the binding of either the CLOSED or OPEN form to actin to make an A-state may be expected to be similar in each case. The isomerization to the R-state seems to require an empty P_i site because no R-state has been detected for myosin complexed with ATP, ATPγS, or ADP and the P_i analogs (85). The R-state can be formed in the presence of either ADP ($K_2 = 10$) or pyrophosphate ($K_2 = 2$). Thus the A-state can be formed with any myosin complex, but the isomerization to the R-state is inhibited by a tightly bound P_i. Formation of the R-state is likely to involve opening of the back door (allowing P_i to dissociate if not covalently bound) and then weakening of the nucleotide affinity. The order is important. Thus the A to R isomerization of the CLOSED form/A-state occurs with opening of the backdoor and loss of P_i. Isomerization of the OPEN form depends on the state of the P_i site. With ATP, ATPγS, or ADP.BeF_3 bound, the formation of the R-state will not be allowed. With no nucleotide or ADP bound, the isomerization to the R-state is highly favored.

In summary the crystallographic data provide evidence of two conformations of the myosin in the absence of actin, which we call CLOSED and OPEN. Their properties are summarized in Table 3. The CLOSED form found when myosin is complexed with ADP.V_i and ADP.AlF_4 is the form with the tail in the up (pre-power-stroke) position with switch 2 IN, poised for catalysis and therefore with the back door for P_i release closed. The OPEN form favored by ATPγS, AMPPNP ADP, and ATP (I Rayment, unpublished data) and sometimes by ADP.BeF_3 (e.g. Dy-truncated at M759) has switch 2 OUT and the backdoor open, and therefore catalysis cannot take place. The tail is in the down position or post-power-stroke conformation.

A Third State Is Required

We suggest that both CLOSED and OPEN forms with the γP_i occupied can interact only weakly with actin to form the A-state and that we need at least one more conformation to complete the cycle. Initially, actin must bind to the CLOSED form to give a weakly bound actin (the A-state). Then the complex should proceed to a third form, which should have the following properties (see Table 3): The third state should bind strongly to actin (R-state) with high pyrene-actin fluorescence; the backdoor should be open and with very weak P_i affinity and weak nucleotide affinity (low mant-nucleotide fluorescence); the switch 2 should be out and the converter domain and lever arm in the post-power-stroke down position.

TABLE 3 Properties of states

Property	CLOSED	OPEN	?3rd state?
Nucleotide	Vi/A1F/Bef	ATP/BeF/γS/ PNP/ADP	Actin only
Switch II	IN	OUT	Further out?
Converter/tail	UP	DOWN	DOWN
Backdoor	CLOSED	OPEN	OPEN
Catalysis	Competent/TS	Noncompetent	Noncompetent
Pi affinity	Very tight	Only covalent as γ Pi	Very weak
Fluorescence (W510)	High (M**ADP.Pi)	Low (M*ATP)	Low
Actin binding	Weak A-state	Weak A-state	Strong R-state
Pyr-actin Fl	High	High	Low
Nucleotide binding	Strong	Strong	Weak
mant.ATP/ADP F1	High	High	Low

The difficult question is how the transition between the three states, CLOSED (M.ADP.P_i) to R-state (A.M or A.M.D) to OPEN (M*ATP) to CLOSED, occurs. The crystal structures allow us to propose that, for OPEN-to-CLOSED transition, the trigger is the moving in of switch 2. At present we have no indications as to how the other two transitions might function. However, solution biochemistry helps set the ground rules. Actin can bind to the CLOSED M**ADP.P_i to form the A-state with no major changes in conformation. The actin then produces a conformational change in the complex which gives a stronger actin binding (R-state sensed by pyrene on actin) and causes the switch 2 to move out (backdoor to open), P_i dissociation, and the converter/tail to move down. Subsequent to this change actin causes a change in the nucleotide site to promote ADP release. This second change can be seen in some slower myosins as an additional tail movement on ADP release (56, 65, 86, 87). ATP binding to AM to return to the M*ATP- OPEN state reverses the A-to-R transition but does relatively little to the converter/tail or to the back door (or switch 2).

A Possible Mechanism for ADP Release

Such speculations allow one to construct a working scheme, but without high-resolution structures of actomyosin complexes they remain conjecture. However, because actin is a nucleotide exchange factor, we could look to other systems involving nucleotide exchange for ideas. A simple structural scenario for the reciprocal relationship between actin displacing ADP and ATP displacing actin is provided by analogy with the G-proteins. For example, the binding of Sos to Ras p21

is accompanied by disruption of the switch-2 region. The Mg^{2+} is forced to leave by the insertion of a methyl group in its place (88). For Tu-Ts the mechanism is different, but one aspect is the same—the binding site for the Mg^{2+} is destroyed (89). In the empty site of F1 ATPase, the Mg^{2+} coordination is also destroyed (44).

Thus nucleotide release in actomyosin could work through weakening the coordination of Mg^{2+}. In myosin, ATP binds with a tightly bound Mg^{2+}, which is then coordinated via bonds with SkD463 and the β- and γ-phosphate groups. After hydrolysis and P_i release, the Mg^{2+} coordination is weakened. It is possible that, after P_i dissociation, actin moves switch 2 and D463 further out, thereby further weakening the Mg^{2+} coordination and resulting in a loss of Mg^{2+} and then ADP. As ATP rebinds with tightly coordinated Mg^{2+}, this would restore switch 2 back through its OPEN to CLOSED position, thereby weakening actin affinity.

EFFECTS OF STRAIN ON PHOSPHATE AND ADP AFFINITY

The above scenario is based on the events in a solution or in an unloaded system. It is of interest to consider the sequence for a loaded motor. Starting from state CLOSED (M**ADP.P_i weak actin binding), actin induces backdoor opening and allows P_i release. Most consider that the major conformation change accompanying force generation occurs before P_i release (81, 90, 91), so we assume that actin binds strongly to the myosin, opening the backdoor and swinging the converter domain, which then allows P_i to dissociate. In the absence of load this goes to the completion of the power stroke and then ADP is lost. If the system is held isometric then either the swing of the tail is arrested or the strain involved in the swing is stored in the head. This has the effect of allowing the P_i to bind reversibly to the myosin head. The open back door and presence of the P_i, however, prevent ADP release. Apparently the swing of the tail (or the dissipation of the strain in the head) is required before actin can cause disruption of the Mg coordination and allow ADP dissociation.

There has long been recognition of the necessity for a strain-dependent ADP release mechanism in actomyosin contraction. This goes back to the Fenn effect and the observations that, without such a mechanism, the observed fast ADP release followed by ATP binding would very rapidly eliminate any strained or unstrained heads in fast skeletal muscles. Smith & Geeves (92) speculated that the ADP pocket might be positioned on the head in such a way that any load on the head could act to close the nucleotide pocket. Based on the analysis of fast skeletal muscles, they further argued that the fast release of ADP would suggest that any pocket opening required for nucleotide release (or ATP binding) would probably be a transition state. Thus strain would affect the rate of nucleotide binding with little effect on the equilibrium constant. More recently the electron microscopy work of Whittaker et al (56) and Jontes et al (86) has shown that, for the smooth muscle myosin and brush border myosin I, a structural change does take place on ADP binding to actomyosin such that ADP release gives an extra

kick to the tail. From a detailed kinetic analysis Cremo & Geeves (84) argued that thermodynamically the ADP release would be unlikely to contribute to force generation, particularly because at cellular concentrations work would have to be put into the system to release ADP (in much the same way that work has to be done to release ATP from myosin and the F1 ATPase). The arrangement would, however, provide a very good strain-limited ADP release mechanism, particularly for a myosin that is designed for high forces and slow contractions such as the smooth myosin. A similar situation appears to hold for the 130-kDa myosin I from rat muscle. This myosin, like brush border myosin I, has been shown to have a double kick in the laser trap experiment (87) and also has a very high affinity for ADP when complexed to actin. It therefore appears to be a myosin designed for load bearing rather than movement (L Coluccio & M Geeves, in press)

MUTATIONAL ANALYSIS AND SEQUENCE COMPARISONS

General

Further insights into the structure-function relationship for myosin come from studies of changes in the sequence of myosin both from engineered mutations and the study of naturally occurring variants. As with the classical work on hemoglobin, the study of the naturally occurring variants of the myosin molecule provide a wealth of information about which parts of the structure are essential for function and which parts are tolerant. A combination of such structural and functional studies provides information on how the protein is tuned to particular physiological functions.

There are currently 15 known members of the myosin super family (3, 93, 94), all related by a conserved motor domain. Few of these myosins have been examined by anything but sequence analysis or genetic knockouts. Because the cellular function of many myosins is unknown, we cannot anticipate how sequence differences result in changes in biological activity. However analysis of sequence comparisons both between and within families has produced insights into the essential and variable regions of the myosin structure (3, 93, 94). The most detailed analysis has been done on the members of the myosin II family, which show a large general homology but variation in local areas particularly between classes (e.g. fast-, slow-, and smooth-muscle myosins and nonmuscle myosins). Analysis of the variations between species and between classes should be quite revealing.

Alternate Splicing

Variations in myosin II structures expressed within a single species often involve multiple genes and alternate splicing of the myosin heavy chain. Bernstein & Milligan (17) analyzed the sequences of the 12 known *Drosophila* myosins, which are products of a single myosin heavy chain (MHC) gene. These 12

sequences are produced by alternate splices at exons 3, 7, 9, and 11, which have 2, 4, 3, and 5 alternate exons, respectively. Exon 7 (Sk301–335) is near the nucleotide-binding pocket, includes Loop 1, and links with the switch-1 region. Exons 3 (Sk69–116) and 9 [Sk472–528 (include W510 conserved throughout)] flank the essential thiol helices in the 3-dimensional structure. Exon 3 includes the N-terminal β-barrel, which is absent in myosin I and has been suggested to be involved in head-head contacts in heavy meromyosin. Residues 82–101 lie close to the SH1 and the hinge regions. Exon 9 is the loop that links switch 2 to the converter domain and includes the W510, which reports the major OPEN-to-CLOSED conformational change. Exon 11 (Sk724–764) is the major part of the converter domain. To date there has been no structural or functional analysis of these alternate splices, but such studies can be expected to help reveal how the function of the myosin is tuned to specific cellular needs.

Spudich (14) pointed out the potential of sequence comparisons. He noted the variation in the number of light-chain–binding motives (IQ motives) and concluded that different myosins might bind different numbers of light chains. This led him and others to test the lever arm hypothesis by deleting and inserting light-chain–binding sites (discussed above). He also identified the surface loops connecting the 25-to 50- (Loop 1) and 50- to 20- (Loop 2) kDa domains as being different between groups of myosin within the myosin II family. He proposed that, although the head structure is generally highly conserved, variations in Loop 2, located in an actin-binding site, can modulate the interaction with actin and hence the actin-activated ATPase. In contrast variations in Loop 1, near the entrance to the nucleotide-binding pocket, can modulate nucleotide affinity and the rate of ADP release and thereby the shortening velocity. Although it was noted that this assignment of the roles of the two loops was simplistic, as there is probably cross talk between the two loops, it remains a useful hypothesis in our search for the mechanisms of ADP release and actin binding. These ideas have been widely tested by constructing chimeras based on either the *Dictyostelium* myosin II S1 (95–97) or the chicken smooth myosin head (98, 99). Kinetic data show the hypothesis to be broadly correct although a simple separation of the roles' effects is not always maintained, particularly for the smooth-muscle myosin.

Loops

The chimeric constructs of Loops 1 and 2 demonstrated that large loop changes can modulate the properties of myosin. However, these studies have not revealed which properties of the loop are important for determining the properties of the myosin. Two studies have attempted a more systematic approach.

Sweeney et al (99) used the smooth-muscle head expressed in baculovirus to study nine variants of Loop 1 taken from a variety of muscle and nonmuscle myosins. These showed that loop substitutions could produce up to a ninefold inhibition of the rate of ADP release and a 2.7-fold and twofold, respectively,

inhibition of in vitro velocities and ATPases. Although there was in general a correlation between the rate of ADP release and the in vitro motility, as anticipated, the changes were not simply related to the properties of the myosins from which the loops originated. Although changes in the charge and length of the loops did cause changes in the behavior of the expressed protein, the correlation was not simple. The group therefore proposed that the primary property of the loop causing the inhibition of ADP release was the reduced flexibility of the loop. Support for this idea came from several other properties of the myosin heads (either S1 or heavy meromyosin were changed by modifications to the loop), including the rate of ATP binding and the ATP hydrolysis step. The loop links two helices, one connecting to the P-loop and the second to the switch-1 region. Thus Sweeney et al argue that changes in the flexibility of the loop could be communicated to the nucleotide-binding site and might modulate ADP release by a mechanism similar to those discussed above.

Support for the role of Loop 1 controlling ADP release from actomyosin also came from studies of the catch and striated-muscle myosins of the scallop (66). These myosins are coded from a single gene and the only significant change in the myosin S1 is an alternate splice at exons 5 and 6, which includes the Loop-1 region (100). Isolation of the two myosins and the S1 molecules allowed detailed biochemical analysis. The loop changes produced changes in in vitro motility (fivefold) and in the basal and actin-activated ATPase rates (threefold). Detailed transient kinetic analysis revealed that the only events modified by the exon change were a tenfold change in the affinity of ADP for acto-S1 (thought to limit in vitro velocity) and the rate of P_i release. Thus at one level the loop behaves as predicted by Spudich. However, in addition the changes affect the key P_i release step, which is compatible with the idea that the loop communicates with the P_i-binding site. The change in sequence is EEEADQKK for the striated to EPVPNLRA for catch, which would give a change in flexibility as proposed by Sweeney.

Furch et al (97) made a series of systematic changes to the Loop 2 of *Dictyostelium* myosin-truncated S1. They increased the length of the loop by 4 to 20 residues and changed the net charge from -1 to +12. The results show that the binding of ATP to the acto-S1 construct was unaffected by any of the changes, consistent with it having no effect on the nucleotide-binding pocket. Similarly, basal ATPase activity was also unaffected. In contrast, the affinity of the S1 fragment for actin was largely unaffected by length changes but increases in the number of positive charged residues dramatically increased the affinity of actin for the nucleotide-free head (100-fold) and increased the apparent K_m of actin (25-fold) in ATPase measurements. This project resulted in the production of a myosin head which has high affinity (~10 μM in 20 mM KCl) for actin even in the presence of ATP and may therefore prove useful for structural studies of the weakly bound cross-bridge. This myosin may prove particularly useful when combined with point mutations, which greatly reduce the rate of the ATP cleavage (16, 101; see below).

The Hinge

The idea of a lever arm mechanism led naturally to an attempt to locate the site of the fulcrum or pivot point for the lever arm. Both the crystal structure and the dependence of velocity, using in vitro motility assays, on the length of the lever arm indicated the two short helices (Sk691–714) carrying the reactive cysteines at Sk697 and Sk707. The two helices are also of interest because they contain three glycines (Sk699, 703, and 710) often used as hinge points in proteins. In particular SkG699 is at the bend between the two helices, and Huston et al (51) proposed that substitution of SkG699 or SkG710 with bulkier residues might inhibit the conformational changes in this region. Kinose et al (102) prepared the equivalent of an SkG699A mutation in chicken embryonic myosin and showed that it had impaired motility properties. The small yields limited the assays that could be performed to motility assays and actin-activated ATPase assays. Both were reduced (ten- and fivefold, respectively). Kinose et al (102) argued that the impaired motility (which was dominant, i.e. 2% mutant myosin in the presence of 98% wild type gave 50% inhibition of velocity) involved an increase in the residence time bound to actin. This probably represents a longer-lived AM.ADP or AM complex.

Using a random mutagenesis of the *Dictyostelium* myosin II, Patterson et al (103) isolated two myosins with mutations at DyG680V and DyG691C (homologous to Sk699 and Sk710). The expression and isolation of these myosins (and G680A, G691A, and S1-like fragments) allowed a wider range of assays. Mutations at either position reduced velocity in motility assays to 10% and, as in the chicken system, the DyG680V/A mutation was dominant when mixed with wild type, whereas the DyG691C mutant was not. DyG680V had inhibited basal (without actin) ATPase at low temperature yet could be activated by actin, whereas DyG691 had an elevated basal ATPase, which was not activated by actin.

The lack of actin activation of the ATPase is sufficient to account for the reduced motility. Moreover, the nondominant effect on wild-type motility of DyG691C suggests that the mutation accelerates the rate-limiting P_i release step and, in doing so, decouples the P_i release from the power stroke. For G680V, Patterson et al (103) were able to show that the affinity for actin either in the presence of ADP or during ATP turnover was enhanced and therefore concluded that the main effect of the mutation was to produce a longer-lived AMD complex. The longer-lived AMD state can result from a reduced rate of ATP binding to AM, increased binding of ADP to A.M (and slower release of ADP from AM.ADP), or creation of a novel strongly bound actin state.

In a recent study, Batra et al (103a) have constructed the three mutations, DyG680A, DyG684A, and DyG691A, in the M761-2R head fragment of *Dictyostelium* myosin II and have completed a detailed study of the interaction of the mutants with actin and nucleotide. DyG684A is near normal in all of its properties. The ATPase data of G680A and G691A agree with the earlier data. For G691 all actin- and nucleotide-binding properties are normal except the rate of P_i release from myosin, which is accelerated. For G680A many major changes in properties were observed, including 20-fold reduction in the rate of nucleotide

binding to M but not AM, a 10-fold-higher affinity of ADP for M, and 100-fold higher affinity for AM. As predicted by Patterson et al (103), the G680A mutant appears to have a very long-lived AM.ADP state which will account for its ability to inhibit motility even in the presence of wild-type protein.

Switch 1

The functional role of the residues in the switch-1 region of *Dictyostelium* myosin II was examined by alanine scanning (104). The residues in the region Dy233–240 have the sequence NXVSSRFG: Each residue was replaced one at a time by alanine. For each construct the ATPase, the in vitro motility, and nucleotide-binding properties were examined. The results showed that N233 and S237 were essential for nucleotide binding, whereas R238 was essential for the hydrolysis of ATP. The equivalent mutations R238C and R238H have been found in the nonmuscle myosin VII in mice, which results in Ushers syndrome (105). Other mutations produced myosins with moderate impairment of properties but are all functional.

The R245–E468 Salt Bridge

The DyR238 (SkR245 SmR247) residue is of interest as it forms a conserved salt bridge with DyE459 (SkE468 SmE470). Mutation of either residue 238 or 459 produces a myosin incapable of hydrolyzing ATP. In an elegant experiment, Onishi et al (106) made the double mutant SmE470R/R247E in chicken smooth myosin and showed that, although either single mutation resulted in loss of ATPase activity, the ability to hydrolyze ATP was recovered in the double mutant, although motor activity was somewhat impaired.

A mutation at E459 in *Dictyostelium* myosin II was found by Ruppel & Spudich (107) in their screening of random mutations in the 454–486 region of *Dictyostelium* myosin and was classified as a nonhydrolyzer. Three nonhydrolyzer mutations were identified in the screen, E459V, N464K, and E476K. Two of these (E459V and E476K) were expressed in the myosin S1 fragment and characterized in detail (101). The E459V construct was particularly interesting because the rate of ATP binding to M was slowed only fivefold and the ATP affinity remained very high (dissociation rate constant 10^{-5} s^{-1}), whereas the rate of the ATP cleavage step was slowed from 30 s^{-1} to 5×10^{-5} s^{-1}; that is, the lifetime of the M*.ATP state was of the order of 5 hours. Such constructs could prove useful in structural studies in the presence of actin.

Point Mutations of G466

A nearby residue was also examined in chicken smooth muscle SmG468A (equivalent to SkG466 DyG457) (108). This residue was thought to be involved in a rotation to allow the formation of the salt bridge (SkR245, SkE468) and to

make an amide hydrogen bond to the γP_i of ATP. The mutation produced a myosin with greatly reduced ATPase activity and no P_i burst (indicative of a reduced rate of the ATP hydrolysis step), yet it bound actin in an ATP-sensitive manner. It also failed to induce any increase in protein fluorescence on adding ATP to the actin-free myosin. This result demonstrates the central role of this residue in bringing about the transition from OPEN to CLOSED and indicates, furthermore, that the control of actin binding by ATP may proceed by a mechanism not closely correlated with this conformational change.

Cardiomyopathies

Another area that has identified mutations in the myosin head with important physiological consequences is the study of familial cardiomyophathies (for a recent review, see 109). The MYH7 gene, which codes for the myosin heavy chain found in cardiac and slow-twitch muscle, has been extensively characterized, and 29 mutations have been located in myosin, of which 24 are in the head region. The head mutations are clustered in four key sites: the actin-binding site, the nucleotide-binding site, the area close to the essential thiol hinge region, and at the head–light-chain interface (110). Few of these mutations have been characterized in detail, and in most cases an interpretation of the effects on the head function is not possible.

Many of the mutations result in dysfunctional myosin and disrupted sarcomeric structures. For such mutations the myosin cannot be easily isolated, although equivalent mutations can be expressed in mouse cell lines (111, 112), in myotubes (113–116), or in *Dictyostelium* myosin. The first mutation ever analyzed, R403 (sk405), which is an actin-binding loop, has been expressed in the equivalent mouse gene (111, 112), R403 (sk405), and R247 (skR249) in cardiomyotubes or quail myotubes (113, 114, 116). The following mutations have been characterized in isolated fibers or in vitro motility assays, and all show reduced motility: T124I (skT125), Y162C (skY163), R247Q (skR249), G256E (skG258), R403Q (R405), R453C (skR445), and V606M (skV607) (117, 118); R719Q (skK721) shows increased motility (119). G741R and R403Q give reduced velocity and lower force (120). The locations of the mutations are marked on Table 1. When expressed in the equivalent positions in *Dictyostelium*, R403Q, F513C, G584R, G716Q, and R719W (121) all show decreased function in solution.

Mutations Should Aid Functional Analysis

The study of point mutations in the myosin molecule is really only just beginning. Although few mutations have yet been characterized in enough detail to interpret their structural and functional significance, such studies already provide clues as to which are important areas of the myosin molecule. Expression of the equivalent mutations in amenable hosts will allow a more thorough examination of the solution properties. Moreover, in the near future one expects that the

mechanical properties will become available from single molecule assays. Only very recently has our understanding of the function of this molecule reached a level where one can begin to integrate the effects of mutations. However, with increasing awareness one can expect that point mutations, both natural and synthetic, will add greatly to our understanding of the role of the different parts of the structure and in particular help define the pathways of information transfer between the different functional regions.

LITERATURE CITED

1. Block SM. 1996. *Cell* 87:151–57
2. Cooke R. 1995. *FASEB* J. 9:636–42
3. Cope TV, Whisstock J, Rayment I, Kendrick-Jones J. 1996. *Structure* 4: 969–87
4. Geeves MA, Conibear PB. 1995. *Biophys. J.* 68:S199–201
5. Goldman YE. 1998. *Cell* 93:1–4
6. Gulick AM, Rayment I. 1997. *BioEssays* 19:561–69
7. Holmes KC. 1998. *Novartis Found. Symp.* 213:76–92
8. Holmes KC. 1997. *Curr. Biol.* 7: R112–118
9. Huxley AF. 1974. *J. Gen. Physiol.* 243: 1–43
10. Huxley HE. 1969. *Science* 164:1356–66
11. Jontes JD. 1995. *J. Struct.* Biol. 115: 119–43
12. Milligan RA. 1996. *Proc. Natl. Acad. Sci. USA* 93:21–26
13. Rayment I, Smith C, Yount RG. 1996. *Annu. Rev. Physiol.* 58:671–702
14. Spudich JA. 1994. *Nature* 372:515–18
15. Spudich JA, Finer J, Simmons B, Ruppel K, Patterson B, Uyeda T. 1995. *Cold Spring Harbor Symp. Quant. Biol.* 60: 783–91
16. Ruppel KM, Spudich JA. 1996. *Annu. Rev. Cell Dev. Biol.* 12:543–73
17. Bernstein SI, Milligan RA. 1997. *J. Mol. Biol.* 271:1–6
18. Smith CA, Rayment I. 1996. *Biophys. J.* 70:1590–602
19. Lymn RW, Taylor EW. 1971. *Biochemistry* 10:4617–24
20. Huxley HE, Holmes KC. 1997. *J. Synchrotron Radiat.* 4:366–79
21. Huxley HE, Simmons RM, Faruqi AR, Kress M, Bordas J, Koch MHJ. 1981. *Proc. Natl. Acad. Sci. USA* 78:2297–301
22. Irving M, Lombardi V, Piazzesi G, Ferenczi MA. 1992. *Nature* 357:156–58
23. Cooke R. 1986. *CRC Crit. Rev. Biochem.* 21:53–118
24. Sabido-David C, Hopkins SC, Saraswat LD, Lowey S, Goldman YE, Irving M. 1998. *J. Mol. Biol.* 279:387–402
25. Kabsch W, Mannherz HG, Suck D, Pai EF, Holmes KC. 1990. *Nature* 347:37–44
26. McLaughlan PJ, Gooch JT, Mannherz HG, Weeds AG. 1993. *Nature* 364:685–92
27. Schutt CE, Myslik JC, Rozycki MD, Goonesekere NCW, Lindberg U. 1993. *Nature* 365:810–16
28. Holmes KC, Popp D, Gebhard W, Kabsch W. 1990. *Nature* 347:44–49
29. Lorenz M, Poole KJ, Popp D, Rosenbaum G, Holmes KC. 1995. *J. Mol. Biol.* 246: 108–19
30. Chik JK, Lindberg U, Schutt CE. 1996. *J. Mol. Biol.* 263:607–23
31. Margossian SS, Lowey S. 1973. *J. Mol. Biol.* 74:301–11
32. Margossian SS, Lowey S. 1973. *J. Mol. Biol.* 74:313–30
33. Mornet D, Pantel P, Audemard E, Kassab R. 1979. *Biochem. Biophys. Res. Commun.* 89:925–32
34. Rayment I, Rypniewski WR, Schmidt-Base K, Smith R, Tomchick DR, et al. 1993. *Science* 261:50–58

35. Houdusse A, Cohen C. 1996. *Structure* 4: 21–32
35a. Xie X, Harrison D, Schlichting I, Sweet RM, Kalabokis VN, et al. 1994. *Nature* 368: 306–12
36. Rayment I, Holden HM, Whittaker M, Yohn CB, Lorenz M, et al. 1993. *Science* 261: 58–65
37. Schroeder RR, Manstein DJ, Jahn W, Holden H, Rayment I, et al. 1993. *Nature* 364:171–74
38. Waller GS, Ouyang G, Swafford J, Vibert P, Lowey S. 1995. *J. Biol. Chem.* 270: 15348–52
39. Kuhlman PA, Bagshaw CR. 1998. *J. Muscle Res. Cell Motil.* 19:491–504
40. Fisher AJ, Smith CA, Thoden JB, Smith R, Sutoh K, et al. 1995. *Biochemistry* 34: 8960–72
41. Smith CA, Rayment I. 1996. *Biochemistry* 35:5404–17
42. Gulick AM, Bauer CB, Thoden JB, Rayment I. 1997. *Biochemistry* 36:11619–28
43. Bohm A, Gaudet R, Sigler PB. 1997. *Curr. Opin. Biotechnol.* 8:480–87
44. Abrahams JP, Leslie AG, Lutter R, Walker JE. 1994. *Nature* 370:621–28
45. Yount RG, Cremo CR, Grammer JC, Kerwin BA. 1992. *Philos. Trans. R. Soc. London Ser. B* 336:55–60
46. Kurzawa SE, Manstein DJ, Geeves MA. 1997. *Biochemistry* 36:317–23
47. Dominguez R, Freyzon Y, Trybus KM, Cohen C. 1998. *Cell* 94:559–71
48. Yount RG, Lawson D, Rayment I. 1995. *Biophys. J.* 68:S47–49
49. Pate E, Naber N, Matuska M, Franks-Skiba K, Cooke R. 1997. *Biochemistry* 36:12155–66
50. Holmes KC. 1996. *Curr. Opin. Struct. Biol.* 6:781–89
51. Huston EE, Grammer JC, Yount RG. 1988. *Biochemistry* 27:8945–52
52. Burgess SA, Walker ML, White HD, Trinick J. 1997. *J. Cell Biol.* 139:675–81
53. Pollard TD, Bhandari D, Maupin P, Wachstock D, Weeds A, Zol H. 1993. *Biophys. J.* 64:454–71
54. Walker M, Trinick J, White H. 1995. *Biophys. J.* 68:S87–91
55. Jontes JD, Milligan RA, Pollard TD, Ostap EM. 1997. *Proc. Natl. Acad. Sci. USA* 94:14332–37
56. Whittaker M, Wilson-Kubalek EM, Smith JE, Faust L, Milligan RA, Sweeney HL. 1995. *Nature* 378:748–51
57. Irving M, Allen TS, Sabido-David C, Craik JS, Brandmeier B, et al. 1995. *Nature* 375:688–91
58. VanBuren P, Waller GS, Harris DE, Trybus KM, Warshaw DM, Lowey S. 1994. *Proc. Natl. Acad. Sci. USA* 91:12403–7
59. Uyeda TQP, Abramson PD, Spudich JA. 1996. *Proc. Natl. Acad. Sci. USA* 93: 4459–64
60. Anson M, Geeves MA, Kurzawa SE, Manstein DJ. 1996. *EMBO J.* 15:6069–74
61. Trentham DR, Eccleston JF, Bagshaw CR. 1976. *Q. Rev. Biophys.* 9:217–81
62. Ritchie MD, Geeves MA, Woodward SK, Manstein DJ. 1993. *Proc. Natl. Acad. Sci. USA* 90:8619–23
63. Marston SB, Taylor EW. 1980. *J. Mol. Biol.* 139:573–600
64. Ostap EM, Pollard TD. 1996. *J. Cell Biol.* 132:1053–60
65. Jontes JD, Milligan RA. 1997. *J. Cell Biol.* 139:683–93
66. Kurzawa-Goertz SE, Perreault-Micale CL, Trybus KM, Szent-Gyorgyi AG, Geeves MA. 1998. *Biochemistry* 37: 7517–25
67. Burghardt TP, Garamszegi SP, Park S, Ajtai K. 1998. *Biochemistry* 37:8035–47
68. Bagshaw CR, Trentham DR. 1973. *Biochem. J.* 133:323–28
69. Millar NC, Howarth JV, Gutfreund H. 1987. *Biochem. J.* 248:683–90
70. Kodama T. 1985. *Physiol. Rev.* 65: 467–551
71. Bagshaw CR, Trentham DR, Wolcott RG, Boyer PD. 1975. *Proc. Natl. Acad. Sci. USA* 72:2592–96
72. Webb MR, Trentham DR. 1981. *J. Biol. Chem.* 256:10910–16

73. Dale MP, Hackney DD. 1987. *Biochemistry* 26:8365–72
74. Taylor EW. 1991. *J. Biol. Chem.* 266: 294–302
75. Woodward SK, Eccleston JF, Geeves MA. 1991. *Biochemistry* 30:422–30
76. Coates JH, Criddle AH, Geeves MA. 1985. *Biochem. J.* 232:351–56
77. Geeves MA. 1991. *J. Cell Sci. Suppl.* 14: 31–35
78. Geeves MA, Gutfreund H. 1982. *FEBS Lett.* 140:11–15
79. Geeves MA. 1989. *Biochemistry* 28: 5864–71
80. Geeves MA, Goody RS, Gutfreund H. 1984. *J. Muscle Res. Cell Motil.* 5:351–61
81. Fortune NS, Geeves MA, Ranatunga KW. 1991. *Proc. Natl. Acad. Sci. USA* 88: 7323–27
82. Geeves MA. 1992. *Philos. Trans R. Soc. London Ser. B* 336:63–70
83. Siemankowski RF, White HD. 1984. *J. Biol. Chem.* 259:5045–53
84. Cremo CR, Geeves MA. 1998. *Biochemistry* 37:1969–78
85. Geeves MA, Jeffries TE. 1988. *Biochem. J.* 256:41–46
86. Jontes JD, Wilson-Kubalek EM, Milligan RA. 1995. *Nature* 378:751–53
87. Veigel C, Coluccio LM, Jontes JD, Sparrow JC, Milligan RA, Molloy JE. 1999. *Nature* 398:530–33
88. Boriacksjodin PA, Margarit SM, Barsagi D, Kuriyan J. 1998. *Nature* 394:337–43
89. Kawashima T, Berthet-Colominas C, Wulff M, Cusack S, Leberman R. 1996. *Nature* 379:511–18
90. Dantzig JA, Goldman YE, Millar NC, Lacktis J, Homsher E. 1992. *J. Physiol.* 451:247–78
91. Kawai M, Halvorson HR. 1991. *Biophys.* J. 59:329–42
92. Smith DA, Geeves MA. 1995. *Biophys. J.* 69:538–52
93. Mermall V, Post PL, Mooseker MS. 1998. *Science* 279:527–33
94. Sellers JR, Goodson HV, Wang F. 1996. *J. Muscle Res. Cell Motil.* 17:7–22
95. Uyeda TQP, Ruppel KM, Spudich JA. 1994. *Nature* 368:567–69
96. Murphy CT, Spudich JA. 1998. *Biochemistry* 37:6738–44
97. Furch M, Geeves MA, Manstein DJ. 1998. *Biochemistry* 37:6317–26
98. Rovner AS, Freyzon Y, Trybus KM. 1997. *J. Muscle Res. Cell Motil.* 18: 103–10
99. Sweeney HL, Rosenfeld SS, Brown F, Faust L, Smith J, et al. 1998. *J. Biol. Chem.* 273:6262–70
100. Perreault-Micale CL, Kalabokis VN, Nyitray L, Szent-Gyorgyi AG. 1996. *J. Muscle Res. Cell Motil.* 17:543–53
101. Friedman AL, Geeves MA, Manstein DJ, Spudich JA. 1998. *Biochemistry* 37: 9679–87
102. Kinose F, Wang SX, Kidambi US, Moncman CL, Winkelmann DA. 1996. *J. Cell Biol.* 134:895–909
103. Patterson B, Ruppel KM, Wu Y, Spudich JA. 1997. *J. Biol. Chem.* 272:27612–17
103a. Batra R, Geeves MA, Manstein DJ. 1999. Biochemistry 38:6126–34.
104. Shimada T, Sasaki N, Ohkura R, Sutoh K. 1997. *Biochemistry* 36:14037–43
105. Well D, Blanchard S, Kaplan J, Guilford P, Gibson F, et al. 1995. *Nature* 374: 60–61
106. Onishi H, Kojima S, Katoh K, Fujiwara K, Martinez HM, Morales MF. 1998. *Proc. Natl. Acad. Sci. USA* 95:6653–58
107. Ruppel KM, Spudich JA. 1996. *Mol. Biol. Cell* 7:1123–36
108. Onishi H, Morales MF, Kojima S, Katoh K, Fujiwara K. 1997. *Biochemistry* 36: 3767–72
109. Bonne G, Carrier L, Richard P, Hainque B, Schwartz K. 1998. *Circ. Res.* 83: 580–593
110. Rayment I, Holden HM, Sellers JR, Fananapazir L, Epstein ND. 1995. *Proc. Natl. Acad. Sci. USA* 92:3864–68
111. Geisterfer-Lowrance AA, Christe M, Conner DA, Ingwall JS, Schoen FJ, et al. 1996. *Science* 272:731–34

112. Vikstrom KL, Factor SM, Leinwand LA. 1996. *Mol. Med.* 2:556–67
113. Watkins H, Seidman CE, Seidman JG, Feng HS, Sweeney HL. 1996. *J. Clin. Invest.* 98:2456–61
114. Marian AJ, Yu QT, Mann DL, Graham FL, Roberts R. 1995. *Circ. Res.* 77: 98–106
115. Marian AJ, Zhao G, Seta Y, Roberts R, Yu QT. 1997. *Circ. Res.* 81:76–85
116. Becker KD, Gottshall KR, Hickey R, Perriard JC, Chien KR. 1997. *J. Cell Biol.* 137:131–40
117. Sata M, Ikebe M. 1996. *J. Clin. Invest.* 98:2866–73
118. Cuda G, Fananapazir L, Epstein ND, Sellers JR. 1997. *J. Muscle Res. Cell Motil.* 18:275–83
119. Poetter K, Jiang H, Hassanzadeh S, Master SR, Chang A, et al. 1996. *Nat. Genet.* 13:63–69
120. Lankford EB, Epstein ND, Fananapazir L, Sweeney HL. 1995. *J. Clin. Invest.* 95: 1409–14
121. Fujita H, Sugiura S, Momomura S, Omata M, Sugi H, Sutoh K. 1997. *J. Clin. Invest.* 99:1010–15
122. Lorenz M, Popp D, Holmes KC. 1993. *J. Mol. Biol.* 234:826–36
123. Esnouf RM. 1997. *J. Mol. Graph.* 15: 132–34
124. Merritt EA, Bacon DJ. 1997. *Methods Enzymol.* 277:505–24
125. Nicholls A, Sharp KA, Honig B. 1991. *Proteins* 11:281–96